Marine Geology 430 (2020) 106336

Contents lists available at ScienceDirect

Marine Geology

journal homepage: www.elsevier.com/locate/margo

Invited research article

Sediment export and impacts associated with river delta channelization compound estuary vulnerability to sea-level rise, Skagit River Delta, Washington, USA

E.E. Grossman[a,*], A.W. Stevens[b], P. Dartnell[b], D. George[b], D. Finlayson[c]

[a] U.S. Geological Survey, Pacific Coastal and Marine Science Center, Dept of Geology, Western Washington University, Bellingham, WA 98225, USA
[b] U.S. Geological Survey, Pacific Coastal and Marine Science Center, Santa Cruz, CA 95060, USA
[c] Chesapeake Technologies, Mountain View, CA, USA

ARTICLE INFO

Keywords:
River delta
Historical change
Channelization
Sedimentation
Progradation
Bathymetry
Tide flats
Marsh
Stratigraphy
Skagit River
Washington
USA

ABSTRACT

Improved understanding of the budget and retention of sediment in river deltas is becoming increasingly important to mitigate and plan for impacts expected with sea level rise. In this study, analyses of historical bathymetric change, sediment core stratigraphy, and modeling are used to evaluate the sediment budget and environmental response of the largest river delta in the U.S. Pacific Northwest to western land-use change beginning in ~1850. An estimated 142 ± 28 M m^3 of sediment accumulated offshore of the emergent Skagit River delta in Washington State between 1890 and 2014 and ~68% of which was found in sand deposits. The fraction of sediment retained in sand reservoirs represents 83% of the expected fluvial sand delivery over this time suggesting their potential utility to evaluate the relative contribution of different land uses to sediment runoff through time. A significantly higher ratio of sand retention to delivery during the period 1890–1939 coincided with extensive watershed denudation (clear-cut logging) and channel dredging, relative to the period 1940–2014, which was characterized by improved forest practices and sediment management to protect endangered species but also more extensive river channelization. Retention in the delta foreset of 78% of the sand delivered by the river between 1890 and 1939 was associated with extensive sediment bypassing and delta progradation that is shown to be 5–10x higher than rates over the Holocene. Comparable offshore sand retention over time and higher nearshore retention subsequent to 1940 after normalizing for the assumed reduction in sediment runoff with improved forest practices, suggests that channelization has continued to influence sediment export at a magnitude equivalent to the effects of early logging. Adverse impacts of the bypassing sediment regime to natural hazards risk and ecosystem management concerns are discussed, including the role of the lost sediment as a resource to mitigate subsiding coastal lands vulnerable to flood impacts. The sediment budget and coastal change analyses provide a framework for evaluating opportunities to achieve greater resilience across several sectors of coastal land use important in low-lying deltas worldwide.

1. Introduction

River deltas, estuaries, and tidal marshes around the world that are critical to global biodiversity, human habitation, and socioeconomic security are facing accelerated and potentially irreparable impacts from human land-use activities, sea-level rise, and climate change (Barnosky et al., 2012; Cardinale et al., 2012; Nicholls and Cazenave, 2010; Steffen et al., 2015). The extent to which future risk and resilience strategies are linked to past sediment management is poorly constrained. Although most of the world's modern deltas initially formed about 6,000 years ago as post-glacial sea level stabilized (Stanley and Warne, 1994), human activities have altered the hydrology and sediment flux to deltas sufficiently that few "reference" systems remain to quantify the extent of human disturbance and guide recovery and protection of delta systems (Wang et al., 2008). Improved understanding of sediment budgets, transport processes, and landscape-scale geomorphic responses to climate and land-use change are therefore critical to mitigate natural hazards risk, protect and restore ecosystems, and implement adaptation planning that promotes resilience (Syvitski et al., 2009).

Studies of human impacts to river deltas have generally found that land use activities including extensive deforestation, use of fire for

* Corresponding author.
E-mail addresses: egrossman@usgs.gov (E.E. Grossman), astevens@usgs.gov (A.W. Stevens), davidf@chesapeaketech.com (D. Finlayson).

https://doi.org/10.1016/j.margeo.2020.106336
Received 9 November 2017; Received in revised form 26 August 2020; Accepted 31 August 2020
Available online 06 September 2020
0025-3227/

clearing, and hydrologic modifications over the last 3000 years led to increased sediment flux to the world's coasts (Syvitski et al., 2009; Anthony et al., 2014; Nienhuis et al., 2020; Wu et al., 2020), whereas improved forest practices and sediment trapping associated with the proliferation by hydropower and flood-control reservoirs have led to significantly reduced sediment flux since ~1950 (Chu et al., 2009; Wang et al., 2007, 2008; Syvitski et al., 2005; Vörösmarty et al., 2003). Relatively strong quantitative data exists characterizing increased sediment fluxes and downstream impacts from activities like deforestation and large-scale mining (Wright and Schoellhamer, 2004; Moftakhari et al., 2015), however few studies (e.g., Wright and Schoellhamer, 2004; Goisan et al., 2013) have quantitatively evaluated the role of channelization in elevating sediment flux and the resulting impacts to coastal and offshore environments. For example, the effects of levees on reducing floodplain connectivity, critical for fisheries and sediment delivery to furnish soil nutrients and compensate for subsidence impacting agriculture, are well understood. Significantly less quantitative information exists to evaluate the costs of levees and channelization to coastal ecosystems and services and resilient long-term flood protection strategies despite the importance of sediment to coastal and marsh stability and hazards mitigation, fisheries and food production, and recreation (Lotze et al., 2006; Kirwan and Megonigal, 2013; Weston, 2014; Ganju et al., 2017). An improved understanding of sediment processes is becoming increasingly important to address expected impacts associated with projected sea-level rise, climate change, and land-use alterations. It is especially relevant along many coastal areas already challenged by sediment management and will be exacerbated by higher sediment delivery projected with greater and more intense precipitation (Lee et al., 2016). Improved understanding of the influence of sediment across diverse, inter-related sectors of society will enable coordinated strategies to be realized important to resilience along the world's coastlines.

This study examines the sediment budget and historical change of a large river delta and the extent that land uses have increased sediment delivery to the coast. It also examines the contribution of flow focusing associated with river-delta channelization to increased sediment export and loss offshore, away from the emergent delta. The results help characterize the complexities and response in sediment routing to the enhanced jet momentum associated with river channelization (Ralston et al., 2013) common along the world's engineered coasts and the resulting vulnerability these systems face. It provides context for understanding recent loss of tidal marsh (Hood et al., 2016) in an estuary with one of the highest fluvial sediment loads along the US West Coast and the potential importance of sediment trapped behind reservoirs for valued coastal ecosystems and their services. The findings help evaluate several adverse impacts of conventional flood- and sediment-management strategies and a framework for investigating river deltas with examples relating the sediment budget and impacts to natural hazards risk management, ecosystem restoration, agricultural resilience, and general adaptation planning, pertinent to temperate estuarine systems worldwide.

2. Study area

The Skagit River delta (Fig. 1) is fed by the moderately large Skagit River that drains a very steep, geologically young watershed extending across 6900 km^2 of the Pleistocene glaciated northern Cascades Range (Booth, 1994). Measurements since the 1970s show that the Skagit River contributes 30–35% of all freshwater and up to 40% of all fluvial sediment delivered to Puget Sound (Curran et al., 2016; Czuba et al., 2011). Maximum daily discharge of the Skagit River at Mt. Vernon ranges 1,400 to 3,680 m^3/s and is characterized by variable autumn and winter rain-fed runoff and generally predictable late spring to early summer snow-melt runoff. The mean annual suspended sediment load of the Skagit River is 2.5 M tonnes; bedload is estimated to be 1-3% of the total load (Curran et al., 2016). Although dams emplaced on the Baker River and upper Skagit River beginning in the 1920s control flow from ~35% of the Skagit watershed area, mass-wasting, historical logging, and retreating snowpack and glaciers in the Sauk and Cascade River watersheds are thought to be the dominant sources of sediment particularly fines that reach the coast (Jaeger et al., 2017; Paulson, 1997). This region of Puget Sound is characterized as meso-tidal with a spring tide range of 3.5 to 4 m. The Skagit River delta is exposed annually to steep waves of 1.0–1.5 m significant wave height and 2–4 sec period (Crosby and Grossman, 2019) and positive storm surge anomalies reaching up to 1 m (Miller et al., 2019), generally during winter (October through April) when rainfall driven run-off and sediment delivery to the coast are highest (Curran et al., 2016).

The Skagit River is the largest salmon producing river delta complex in Puget Sound (Beamer et al., 2005); however, like many other systems in Washington State, it has experienced 80–90% loss of estuarine habitat due to diking and wetland "reclamation" for agriculture and urban expansion since the 1850s (Bortleson et al., 1980). Reconstructions by Collins (2000) showed that the Skagit River historically maintained an extensive network of shallow distributary channels across ~200 km^2 of emergent delta and floodplain delivering water and sediment to Samish, Padilla, and Skagit Bays (Fig. 2A). Removal of large woody debris and side cast dredging between the late 1870s and ~1910 was suspected to have added significant sediment to Skagit Bay and caused sedimentation of the lower distributaries that allowed transit of large steam-powered vessels through the delta to Mount Vernon (USCGS, 1891; Nesbit, 1885; Collins, 1998, 2000). By 1950, an extensive flood-protection levee complex from Burlington to its two present outlets in Skagit Bay reduced flow connectivity to a mere 10% of its past floodplain area (Fig. 2B). Today farming across the Skagit River lowlands contributes 25% of the world's cabbage and beet seed, and ~8% of the world's spinach seed (WSU, 2014).

In the early 1940s, a 4-km jetty was constructed in Skagit Bay to redirect sediment away from and aid navigation through Swinomish Channel, which further restricted the flow of the river. Historical maps and photographs show the flow of the North Fork Skagit River oriented northwest at its mouth in 1937 prior to the jetty and the shoreline and marshes landward of their present positions (Fig. 2C). More recently, aerial photographs showed an extensive network of braided tidal channels extending 4–8 km across the entire tide flats offshore of the channelized North and South Forks in stark contrast to the central tide flats characterized by smooth topography and nearly void of channels or bedforms (Fig. 1). Whereas the export of sediment offshore represents a loss of a resource to the subsiding farm areas of Fir Island and marshes (Fig. 2B) vital for salmon productivity and recovery (Beamer et al., 2005), sediment export is also increasingly a concern for disrupting and fragmenting offshore habitats like seagrass meadows, important in early salmon development (Rubin et al., 2018). This study focuses on the historical change and sediment budget of the Skagit River delta and Bay system between Deception Pass in the north and Camano Island to the south (Fig. 2D). Estimates are made of the change in, and partitioning of, sediment among marsh-, mud- and sand-dominated tide flats, delta front and other sediment reservoirs through time relative to delivery. The resulting budget and evaluation of how modifications to the landscape and sediment transport regime contribute to concerns like subsiding agricultural lands and recent loss of marshes (Hood et al., 2016), despite one of the highest sediment loads in Puget Sound (Czuba et al., 2011), aim to help inform vulnerability and resilience decisions.

3. Materials and methods

3.1. Data acquisition

A combination of high-resolution bathymetry, seismic-reflection profile data, and sediment cores were collected across the Skagit River delta to examine morphology, stratigraphy, and sediment transport

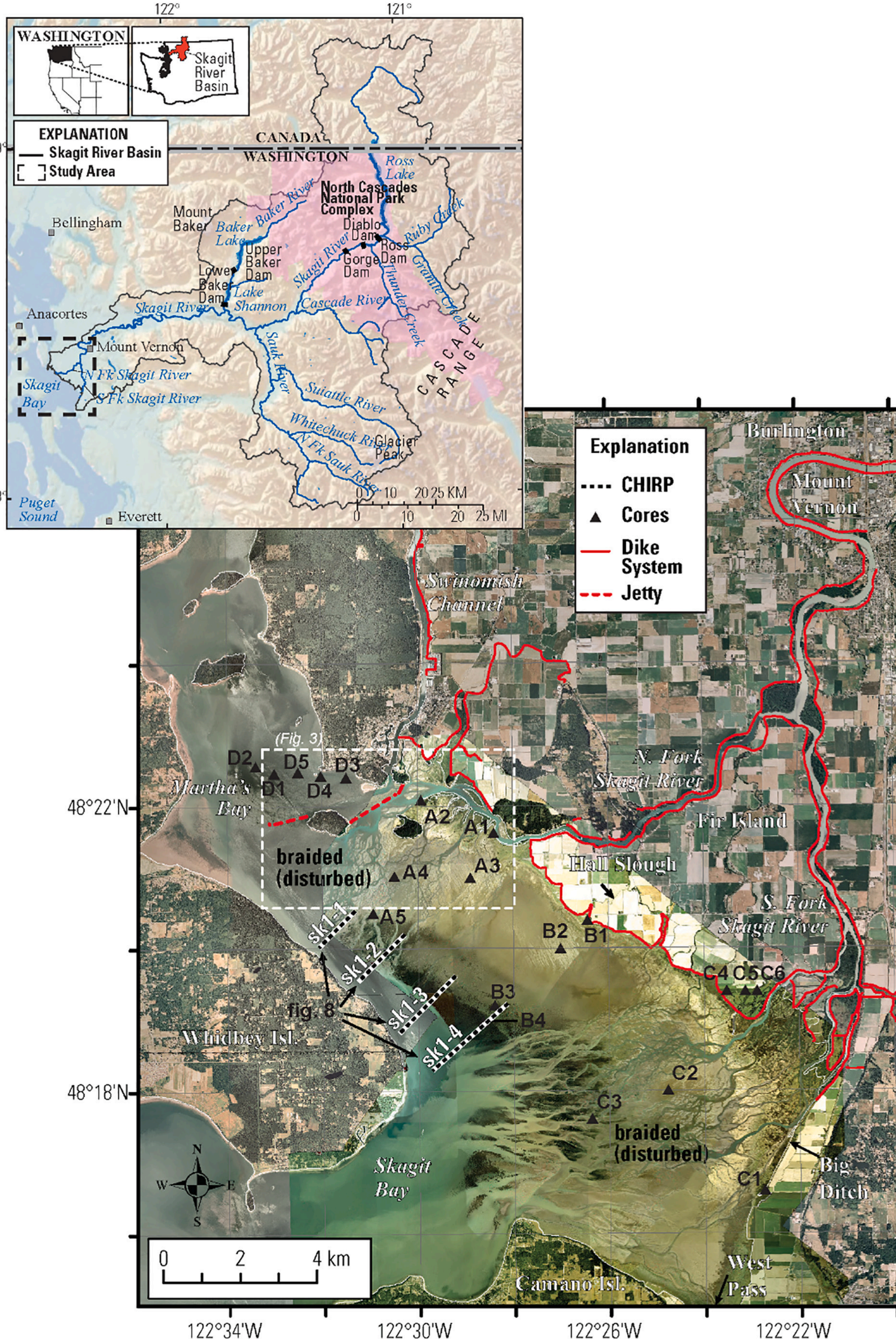

(caption on next page)

Fig. 1. Annotated 2003 aerial photo of the Skagit River delta study area and impounded reservoirs within the watershed (inset) showing sampling sites and transects relative to the levee network. Braided tidal flat channels offshore of the channelized North and South Forks are distinctly different than the less disturbed areas of central Fir Island and Martha's Bay.

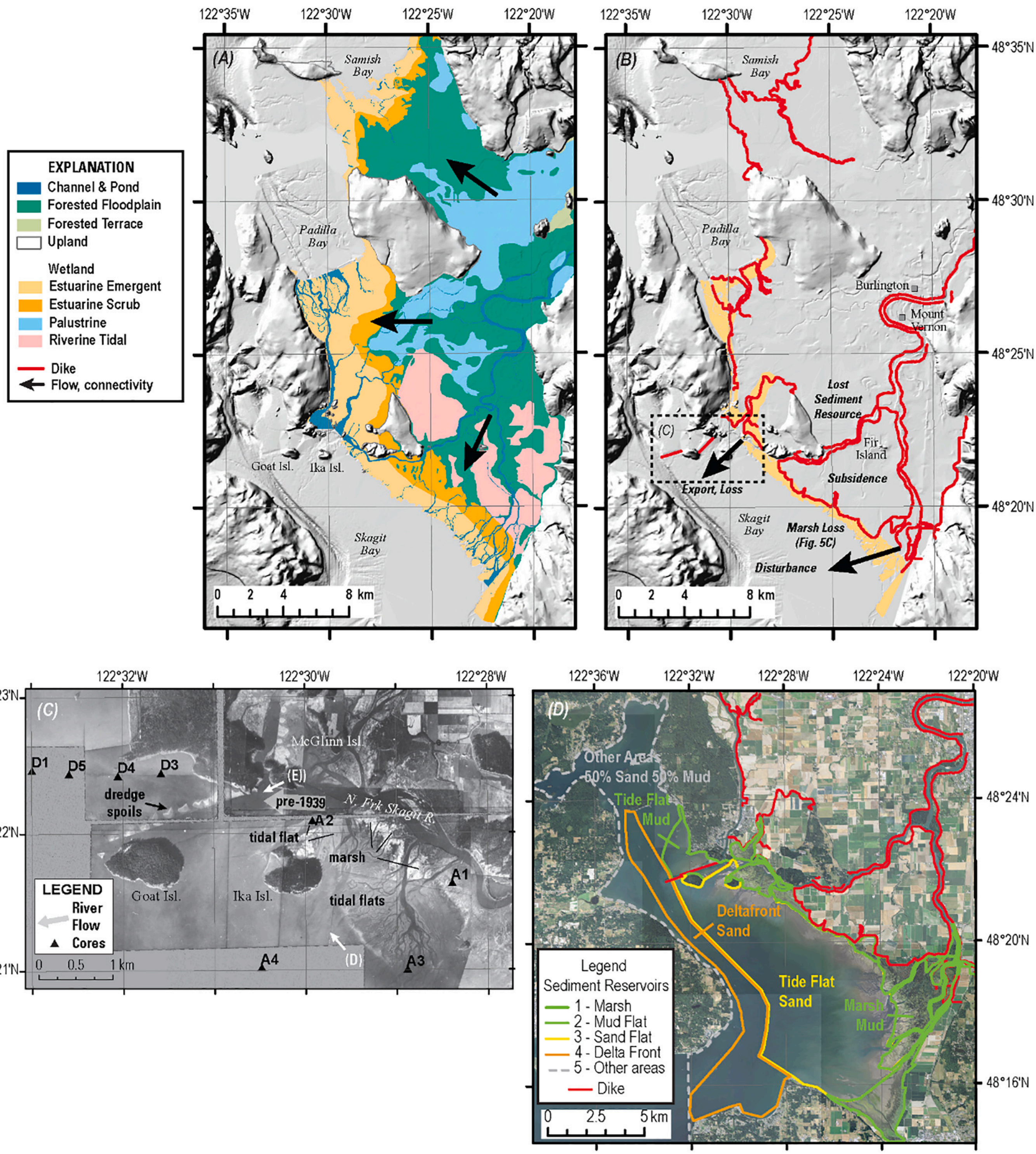

Fig. 2. Annotated map of the 1860 extent of the Skagit River delta, vast wetlands, and connected distributaries (A) that drained to Samish, Padilla and Skagit Bays (arrows) relative to after the network of levees and dikes were completed in 1950, (B) which redirected the entire Skagit River flow and sediment load to its present two outlets (arrows) in Skagit Bay (modified after Collins, 2000). (C) 1937 aerial photo showing the flow path of the North Fork (grey arrow) prior to initial jetty construction in 1939, and location of core sites (location in B). (D) Map showing the sediment reservoirs analyzed in this study.

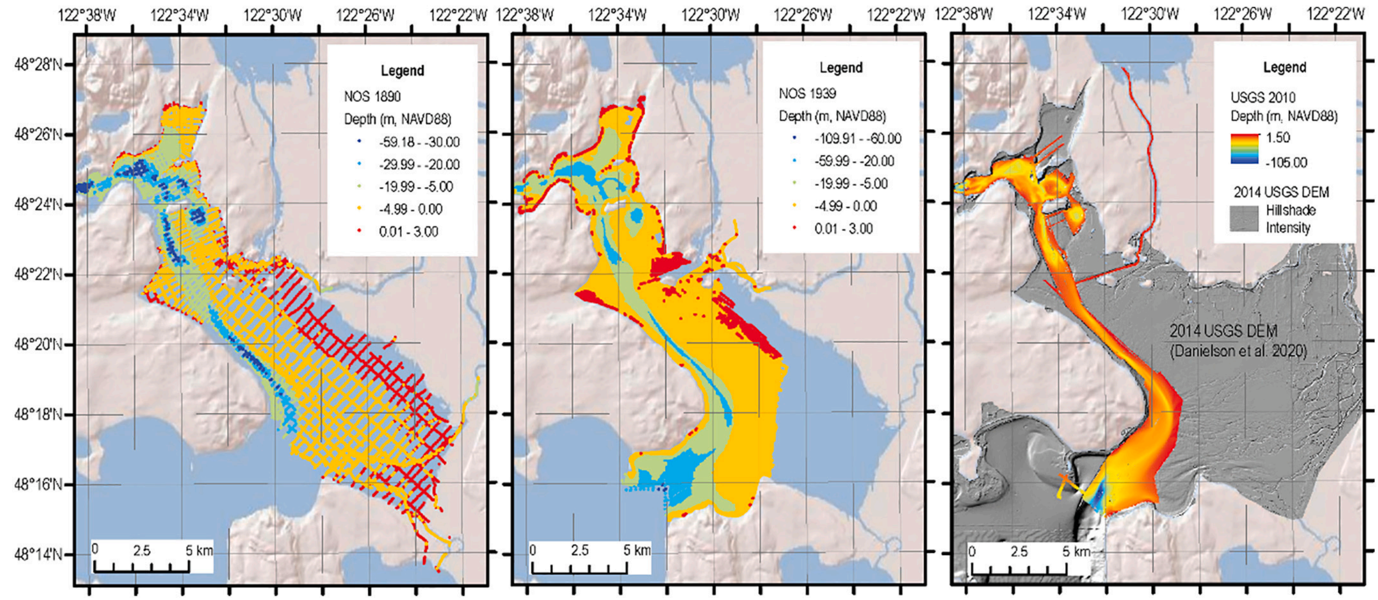

Fig. 3. Map showing the coverage of sounding data from 1890 (A), 1939 (B), and 2010 (C) used to examine change.

processes. High-resolution acoustic 234 kHz swath bathymetry, 200 kHz single-beam bathymetry, and swept-frequency CHIRP seismic-reflection profile data were collected during several surveys between 2005 and 2010 (Figs. 3 and 4); the details of these efforts and results are reported in Grossman et al. (2018). Sediment vibracores, pushcores, and auger cores were collected at 32 sites across the Skagit River delta (Fig. 1, Table 1); the details of these cores are reported in Grossman et al. (2011). Briefly, core penetration ranged 0.4 to 9.6 meters and recovery was typically 90–100%. Cores were cut to 1.2 or 1.5 m lengths for transport to the USGS Sediment Storage Refrigerator in Menlo Park, CA, where they were stored at 4 °C until further processing. In September of 2007, 40 sediment grab samples were collected with a standard 10-inch Van Veen grab along 6 cross-shore transects to field test swath acoustic backscatter and aerial photograph interpretations of substrate type (Fig. 5). Grabs were kept only when recovery was > 80% of the Van Veen capacity but not overfilled and surface texture was undisturbed. Samples were transferred to whirlpacks, labeled, and kept on ice. Occasionally, rock substrate was identified with a defined metallic ring upon reaching the bottom and triplicate attempts lacked recovery.

3.2. Data processing

The swath bathymetry and acoustic backscatter data were collected and processed digitally for altitude, positioning, and sound velocity using SEA software, followed by filtering using Caris software; the details are reported in Grossman et al. (2018). Positions were determined using RTK-GPS with uncertainties of < 5 cm and 10 cm for horizontal and vertical positions, respectively. Filtered swath bathymetric data and the standard deviations of soundings were output at 1-m resolution. An RMS of 0.25 m was derived for the swath data accounting for instrument error, position, and datum uncertainty. Single and dual-frequency bathymetry were processed following Stevens et al. (2008) with an RMS of 0.27 m estimated from tie-line crossings. Elevation surfaces based on near-neighbor interpolation of these data were merged with 2014 topobathymetric lidar (light detection and ranging) data to construct a final digital elevation model (DEM) (Fig. 3) at a resolution of 1 m (Tyler et al., 2020). The CHIRP seismic-reflection profile data were processed, and acoustic reflectors were interpreted and digitized using Triton-Elics Sub-Bottom Interpreter software and output in SEG-Y format and as tiff image curtains. Conversion of travel time to sediment thickness was made using a standard velocity correction of 1750 m/s for the siliciclastic sediment and 1520 m/s for water (Jackson et al., 1996).

Sediment cores were analyzed for physical properties on a Geotek, Ltd, multi-sensor core logger and imaged by x-radiography before visually inspecting and interpreting lithofacies and imaging with standard photography. All subsequent sampling and analyses for particle size and carbon content were made on a working half and reported in Grossman et al. (2011); an archive half remains for future reference. Analyses of ^{14}C wood and shell fragments were conducted at the Lawrence Livermore Laboratory CAMS facility by standard ^{14}C-^{12}C measurements of graphitized samples after removal of detritus observed under a microscope and an 10–15% acid-wash of carbonate samples (Table 2). ^{14}C ages were corrected for isotopic fractionation using measured $\delta^{13}C$ and calibrated to calendar years using the Calib. Software program version 6.0 (http://calib.qub.ac.uk/calib/). Marine samples included a marine reservoir correction of 412 ± 55 years (Stuiver and Reimer, 1993). Vertical accretion rates for core sites analyzed with ^{14}C were derived by dividing the difference in sample depths or core top by the associated difference in ages.

3.3. Historical data

To examine changes in bathymetry, geomorphology, and patterns of sediment accumulation, historical bathymetry data were compared to our 2005–2010 sonar-derived bathymetric data. Sounding data from 1890 (U.S. Coast and Geodetic Survey Hydrographic study USCGS 2050, 1891) and 1939 (NOS surveys H06475, H06476 and H06477) were acquired from the NOAA National Ocean Service (NOS) hydrographic survey data center (http://map.ngdc.noaa.gov) (Fig. 3). Data from 1890 referenced to mean lower low water (MLLW) with a reported vertical uncertainty of 0.15 m in geographic coordinates (WGS83), while 1939 data were referenced to MLLW and NAD83 UTM Zone 10. To assess the potential for large uncertainty associated with the older measurements, the raw soundings were compared over flat, hard (rocky) areas observed in the 2010 bathymetry and backscatter intensity data (Grossman et al., 2018) that are assumed to have changed little since 1890 (Fig. 4B). Comparisons between the 1890, 1939, and 2010 soundings sampled within 10 m of each other over these reference areas were strongly correlated ($n = 44$, $r^2 = 0.99$, P-value of 0.05) and showed a mean difference of 0.30 m with a standard deviation of 0.50

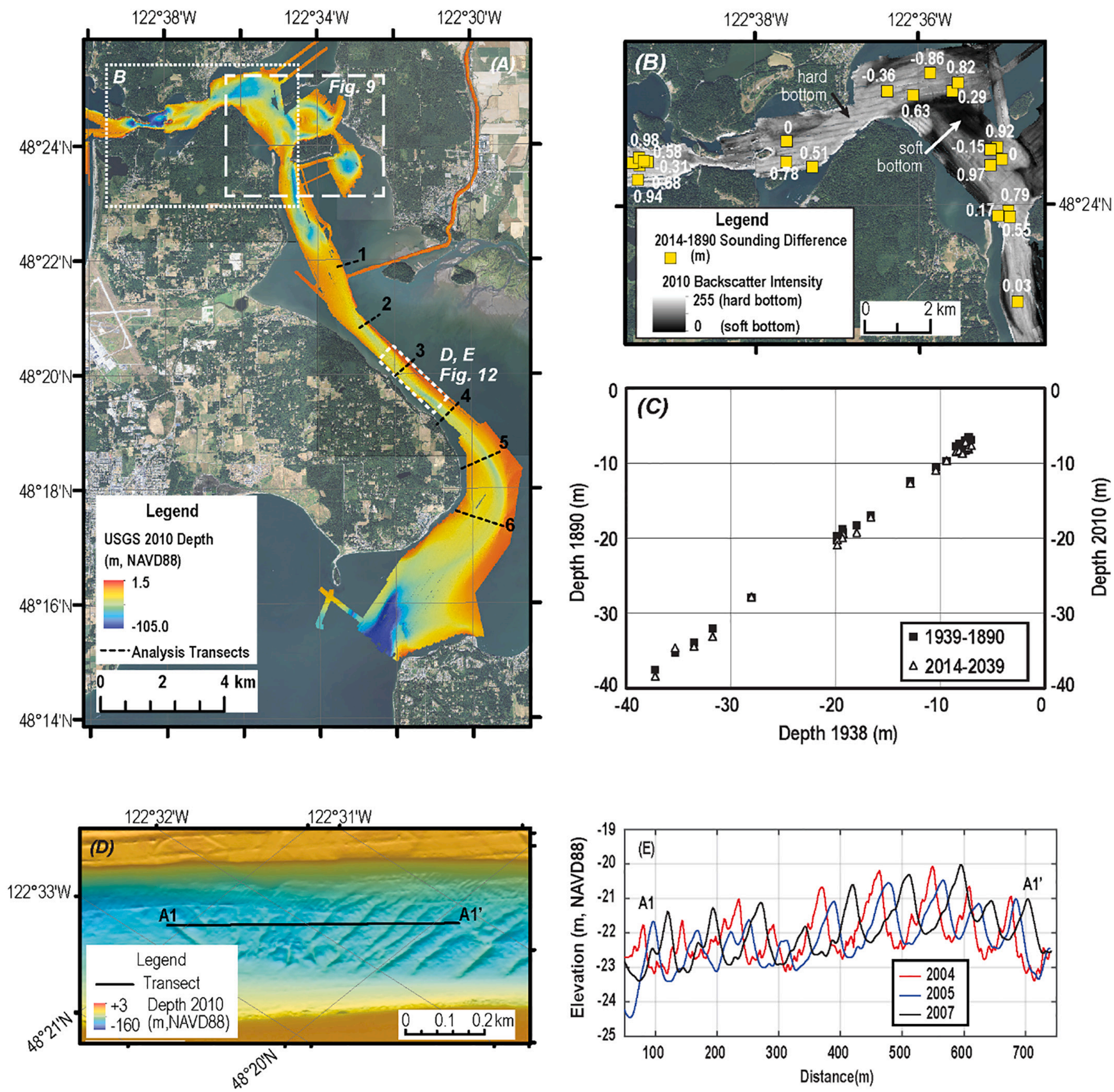

Fig. 4. Map of the high-resolution 2010 bathymetry (A) and area of acoustic backscatter intensity (B) showing where sounding comparison were made over low sloping and hard (rocky) bottom (high intensity) where variations in sedimentation might be minimized. (C) Plot of the 1890, 1939, and 2010 comparison soundings showing consistency within 0.3 ± 0.5m. (D) Map of sandwaves in central Skagit Bay. (E) Plot of sandwave profiles over 3 surveys showing steep lee sides oriented and indicative of bed movement to the south.

m (Fig. 4C). We use the standard deviation as a measure of total uncertainty in change analyses. We corrected the older data to the present tidal epoch assuming the rate of sea level rise of 2 mm/yr as observed at Seattle (NOAA tide station 9447130) since 1900 (https://tidesandcurrents.noaa.gov/sltrends/sltrends_station.shtml?id=9447130). Depth values were transformed to NAVD88 using NOAA VDatum software.

We evaluated the potential error introduced by kriging, triangulated irregular network, and inverse distance weighted interpolation algorithms of the coarser 1890 and 1939 data using a subsample of our integrated 2014 sonar and lidar data with known uncertainty. First, we extracted our 2014 bathymetric data at the 1890 and 1939 sampling positions. Interpolations were conducted on these samples using each of the three methods, and errors were evaluated as the mean differences between the known 2014 surface and the interpolated surfaces. We determined that kriging minimized error due to interpolation, producing mean differences of 0.06 m and 0.10 m between the interpolated grid and known 2014 surface for the 1890 and 1939 sampling regimes, respectively. Comparisons indicated that kriging introduced similar error for each historical data set. Final bathymetric surfaces were generated for all surveys using kriging with fitted linear variograms to interpolate values onto 5 m grids with cells aligned. Errors included reported measurement error and interpolation errors based on the test above.

Table 1
List of sediment core information.

Core ID	Sample Date (UTC)	Latitude	Longitude	Elev (m, MLLW)	Penetration (m)	Recovery (m)
A1-A	03/12/2004 19:00	48.36039	−122.47315	3.94	2.12	2.12
A1-B	03/12/2004 20:00	48.36039	−122.47315	2.69	2.27	2.23
A2	09/09/2004 22:37	48.36805	−122.49872	3.26	3.02	3.00
A3	03/12/2004 22:00	48.34990	−122.48143	0.97	1.60	1.50
A4	09/06/2004 17:30	48.35018	−122.50808	−0.15	1.95	1.95
A5	09/22/2006 20:33	48.34166	−122.51555	−2.41	3.81	3.81
B1	09/10/2004 21:59	48.33994	−122.44053	3.12	2.15	2.15
B2	09/06/2004 20:05	48.33333	−122.45000	1.51	1.84	1.84
B3	09/08/2004 16:23	48.32000	−122.47306	−1.23	3.60	3.60
B4	09/10/2004 16:30	48.31627	−122.47701	−1.53	4.50	4.50
C1	09/05/2004 19:44	48.27669	−122.37889	3.10	1.91	1.91
C2	09/06/2004 21:33	48.30004	−122.41257	0.30	1.82	1.80
C3	09/08/2004 16:20	48.29340	−122.43924	−0.62	3.95	3.95
C4	03/09/2004 16:00	48.32278	−122.39154	2.10	9.60	9.60
C5	03/09/2004 17:30	48.32274	−122.38660	2.10	9.60	9.60
C6	03/09/2004 20:00	48.32273	−122.38205	2.10	9.60	9.60
D1	09/20/2006 17:29	48.37431	−122.54993	−0.19	3.00	3.00
D2	09/21/2006 19:33	48.37638	−122.55591	−0.92	2.40	2.40
D3	09/08/2004 18:44	48.37222	−122.52667	0.75	0.50	0.70
D4	09/08/2004 19:47	48.37516	−122.54240	0.50	0.40	0.45
D5	09/08/2004 19:54	48.37343	−122.53554	0.35	0.40	0.40

3.4. Sediment budget and change analyses

Calculations of the sediment budget and metrics of change including volume change and progradation rates of geomorphic features and sediment reservoirs (Fig. 2D), marsh accretion, retention defined as the ratio of sediment reservoir volume to flux, and potential sedimentation time were derived from the mapping data, core analyses and modeled relationships to existing published data. Bathymetric differencing informed volume changes of the delta front, tide flats, and other areas surveyed and accounted for uncertainty with instrument and sampling, interpolation, and environmental uncertainties that together averaged 10–20% of the volume change. Change in the marsh reservoir was calculated by extrapolating the mean thickness of marsh facies (1.5 m, Table 3) observed in sediment cores across the mapped area of marsh connected hydrologically to the lower river and tides. It includes errors ranging 5–10% associated with mapping, aerial photo rectification and digitization, and core sampling. In addition to bathymetric differencing, the volume change of sand and mud over the tide flats was also calculated extrapolating the thickness of those facies observed in sediment cores over their respective areas. Delta front progradation and vertical accretion rates were calculated accounting for the distance and time that dominant inflection points along the tide flat-delta front slope break and base of the delta slope, respectively, shifted along 6 analyses transects between surveys (Fig. 3A). Errors in these rates reflected location uncertainty and interpolation error but were generally < 5%. Marsh accretion rates were calculated dividing the difference in depth of samples analyzed in cores by the span in time associated with their calibrated ^{14}C ages, as well as from ages of historical aerial photos that document marsh development. Sediment retention was derived by dividing the calculated reservoir volume (and/or mass) change by the estimated sediment delivery whereas a metric referred to as potential sedimentation time converted reservoir volume to time in years dividing by the annual sediment flux based on Curran et al. (2016).

4. Results

4.1. Modern delta morphology and substrate

The 2010 sonar and 2014 DEM data show that the Skagit River delta today is characterized by broad shallow tide flats extending 5 to 8 km seaward of the shoreline to ~1–2 m (NAVD88) where the delta front abruptly descends to the bottom of Skagit Bay which ranges -20 to -30 m (Fig. 4). The average delta front slope ranges 5–8 degrees and is steepest offshore of the present North Fork, where locally the gradient reaches 15–16 degrees. The acoustic backscatter intensity shows a complex distribution of strong reflecting (hard) surfaces found to be bedrock, pavements, or uniform densely packed sands, and weak reflecting (soft) surfaces observed to be mud, mixed sediments or thicker deposits of sand (Fig. 4B; Grossman et al., 2018). Large bedforms are common as observed in central Skagit Bay attesting to the strong circulation in the area (Fig. 4D, E). Marshes along the shoreline outside of the protective dikes and river levees range in elevation of 2.75–3.50 m (NAVD88) (mean of 3.0–3.2 m) perched just above mean higher high water (MHHW, 2.754 m, https://tidesandcurrents.noaa.gov/datums.html?id=9448576).

In the earliest aerial photograph available of 1937 prior to the emplacement of the jetty, the morphology of the tide flats west of Goat Island was considerably less braided than in 2003 (Figs. 1 and 2). Many of the channels observed today adjacent to Goat Island and south of the jetty are not observed in the 1937 photograph. Today, braided channel complexes extend the entire distance from the shoreline to the delta front for a total of 4 km offshore of the North Fork Skagit River and 8 km offshore of the South Fork. In contrast, the tide flats offshore of central Fir Island and north of the jetty in Martha's Bay are smooth and lack meandering channels (Fig. 1). Dark green patches along the outer tide flats observed in true color aerial photographs (Fig. 1) were field-verified through direct sampling to be eelgrass meadows (*Z. marina*) (Gaeckle et al., 2009, McBride et al., 2006, this study). The eelgrass meadows were significantly more fragmented offshore of the North and South Forks Skagit River than the central delta where braided channels were absent.

Sediment grain size results from sediment grabs show that the braided North and South Fork tide flats are composed principally of sand (Fig. 5A). A slight offshore fining occurs across the tide flats, but sands dominate the composition across the tide flats and into central Skagit Bay beyond the delta front. Sediments are coarser across and offshore of the North and South Forks than the central tide flats offshore of Fir Island (Fig. 5B,C) and where erosional marsh pedastals found stranded offshore 300–500 m indicate recent change. This is in stark contrast to the surface substrate of Martha's Bay north of the jetty, where the tide flats are almost entirely covered in mud (Fig. 5D). Sediments along the deep axis of the bay were generally finer North and South of the influence of the North Fork river mouth.

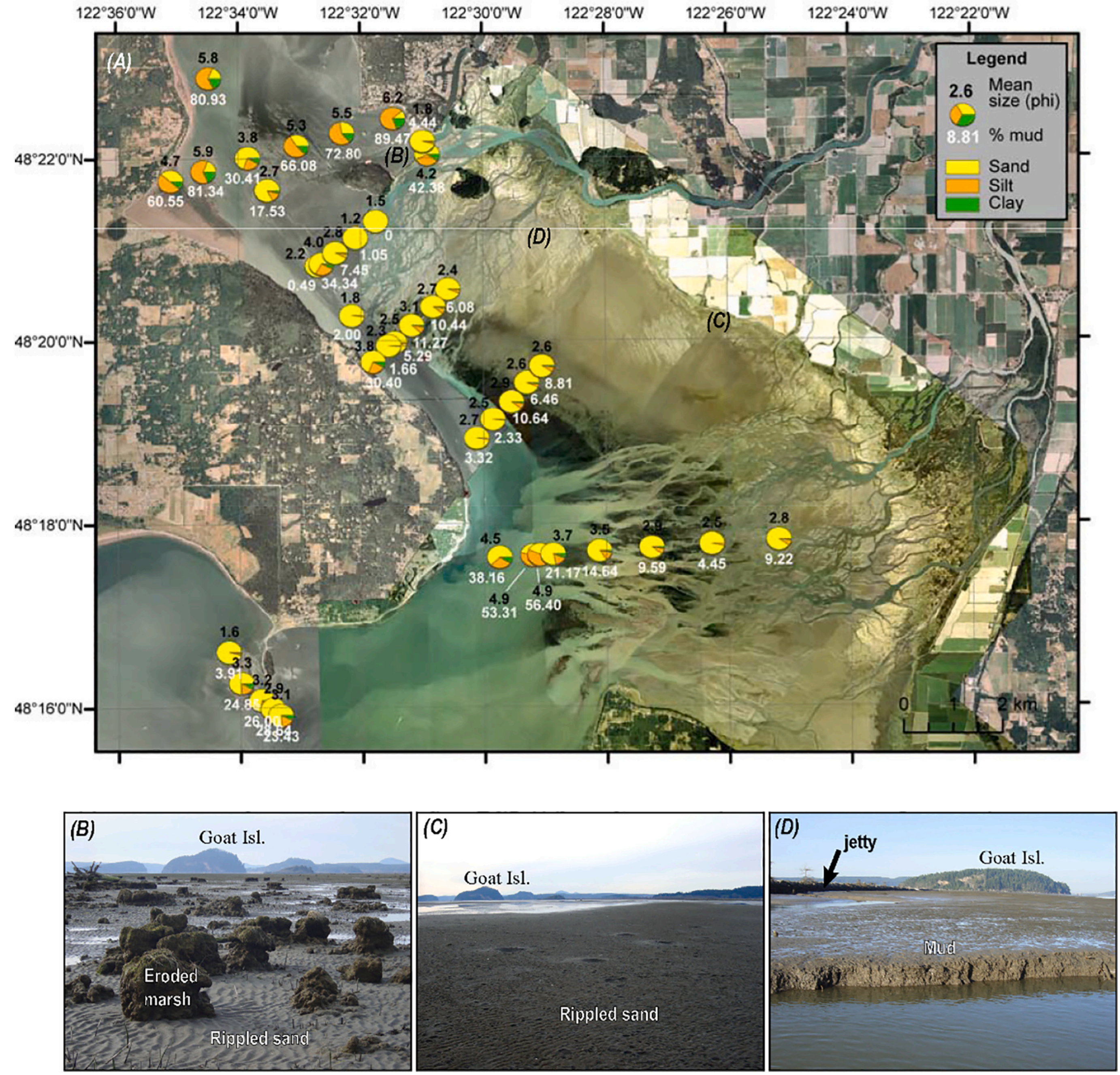

Fig. 5. Map showing surface sediment composition and the coarser nature of substrate across the entire tide flats of the North and South Forks relative to Martha's Bay (A). Photographs of mud accumulation in the lee of the jetty in 2007 (B), eroded marsh pedastals stranded 300–500 m offshore of central Fir Island (C), and the sandy, rippled tidal flat offshore of North Fork (D), locations of photographs in Fig. 2B

4.2. Historical bathymetric change

Comparison of 1890, 1939, and 2014 bathymetry show the progressive progradation of the tide flats and extensive sedimentation of the bay over the last 120 years. The delta progaded seaward up to 690 m since 1890, with a first pulse between 1890 and 1939 west-northwest of Goat Island followed by a second pulse between 1939 and 2014 focused 2–5 km to the south after the jetty was emplaced (Fig. 6A–C, Fig. 7). The 2014 and 1939 bathymetry showed that nearly the entire bay shallowed 5–20 m since 1890. The bathymetric changes over the periods 1890–1939 and 1939–2014 reveal the accumulation of a sediment wedge along 14 km of the delta front that reaches 25–27 m thick in both time intervals (Fig. 6D, E, F, Fig. 7). The mean thickness of this sediment deposit characterized by sand (Fig. 5) ranges 5.5 m. Immediately west of the aggraded sediment wedge, 100–300 m of lateral erosion occurred along the submerged flanks of Whidbey Island and 5–8 m of vertical scour occurred over portions of the Skagit Bay seafloor (Fig. 7). Several metrics of change including volume change, peak and mean vertical accretion rates, and maximum progradation rates of the wedge were greater during the period 1890–1939 than 1939–2014 (Table 3). Both the North and South Forks of the lower Skagit River experienced sedimentation between 1890 and 2014 (Fig. 8A, B). Significant sedimentation was also found farther removed from the two river mouths including up to 20 m in areas characterized by mud (Fig. 8C).

Profiles across the delta front and Skagit Bay reveal the extent that

Table 2
List of $^{14}C_{AMS}$ ages and derived accretion rates from sediment core samples.

SampleID	CAMS#	Core Depth (m)	Elevation (m, MLLW)	Description	δ13C	Fraction Modern	14C Age (yr BP)	Cal Age (yr BP)	Accretion Rate[a] (mm/yr)	Accretion Rate[b] (mm/yr)
A1-1-85	116414	0.85	3.09	wood	−28.824	1.2786 ± 0.0048	modern	modern	-	-
A2-255	116416	2.55	0.71	wood	−25.684	0.9897 ± 0.0029	85 ± 25	84.5 ± 55.5	-	30.18 ± 63.14
A2-295	116417	2.95	0.31	wood	−23.745	0.9448 ± 0.0031	455 ± 30	507 ± 29	0.79 ± 0.39	-
A3-152	116415	1.52	-0.55	wood	−28.771	0.9336 ± 0.0035	550 ± 35	539.5 ± 24.5	-	2.81 ± 0.52
B2-115	116420	1.15	0.36	wood	−25.000	0.9501 ± 0.0036	410 ± 35	474.5 ± 46.5	-	2.42 ± 0.73
B3-120	116418	1.20	−2.43	wood	−30.140	0.9061 ± 0.0042	790 ± 40	722.5 ± 53.5	-	1.66 ± 0.43
B3-330	116419	3.30	−4.53	wood	−25.062	0.8834 ± 0.0029	995 ± 30	931 ± 33	10.10 ± 7.12	-
C2-140	116424	1.40	−1.11	wood	−26.080	0.9797 ± 0.0032	165 ± 30	180.5 ± 49.5	-	7.76 ± 4.46
C3-288	116421	2.88	−3.50	wood	−24.460	0.8742 ± 0.0023	1080 ± 25	973.5 ± 40.5	-	2.96 ± 0.34
C3-288B	116422	2.88	−3.50	shell	−1.324	0.8588 ± 0.0029	1225 ± 30	417 ± 112	-	-
C3-390	116423	3.90	−4.52	wood	−26.387	0.8643 ± 0.0028	1170 ± 30	1111.5 ± 62.5	1.47 ± 0.49	-
C4-457	107078	4.57	−2.47	wood	−25.000	0.8684 ± 0.0033	1135 ± 35	1053 ± 90	-	4.34 ± 0.61
C4-914	107079	9.14	−7.04	wood	−25.000	0.9507 ± 0.0036	405 ± 35	472.5 ± 45.5	-	19.33 ± 2.55
C5-610	107080	6.10	−4.00	wood	−25.000	0.9826 ± 0.0039	140 ± 35	225 ± 56	-	27.09 ± 10.16
C5-610B	107085	6.10	−4.00	shell	0.000	0.8187 ± 0.0031	1605 ± 35	1870 ± 134	-	-
C5-914	107081	9.14	−7.04	wood	−25.000	0.7681 ± 0.003	2120 ± 35	2075.5 ± 81.5	14.8 ± 36.86	-
C6-488	107082	4.88	−2.78	wood	−25.000	0.9516 ± 0.0036	400 ± 35	470.5 ± 44.5	-	10.35 ± 1.56
C6-945	107083	9.45	−7.35	wood	−25.000	0.9817 ± 0.0037	150 ± 35	106.5 ± 47.5	-	-

[a] Accretion rate between dated samples.
[b] Accretion rate based on dated sample to assumed modern core top.

the delta has steepened, patterns of bay sedimentation and fill, and how the axis of the bay thalweg moved westward through time (Fig. 7). In the northern area the tide flats prograded up to 555 m between 1890 and 1939 and the delta front slope steepened near Transect 1 (Fig. 7A). Slight erosion occurred offshore. The next three profiles to the south show a progressive change in the timing and extent of seaward progradation ranging 300–200 m with much more change after 1939. Significant shallowing of Skagit Bay through time (Fig. 7B-D). Along Transects 2 and 3, the delta front has continued to steepen though time. The central Skagit Bay channel thalweg also moved 200 and 300 m westward during this time and was associated with ~100–200 m of incision of the eastern, subtidal flanks of Whidbey Island. In the south-central portion of Skagit Bay, progradation of the delta ranged 200–300 m and vertical filling of the bay ranged 3–10 m (Fig. 7E). In response, the thalweg moved westward ~100–150 m and incision into Whidbey Island occurred at depths above ~12 m (Fig. 7E). Along the southern most profile studied, historical data coverage is limited and change between 1939 and 2014 indicate slight erosion (Fig. 7F)

4.3. Shallow seismic stratigraphy

High-resolution CHIRP seismic reflection profiles reveal that the sediment wedge south of the jetty that formed between 1939 and 2014 and observed in bathymetric change analyses (Fig. 9) is a massive, semi-transparent sediment package that conformably drapes older gently sloping surfaces observed as strong shallow-buried acoustic reflectors dipping away from the delta into Skagit Bay (arrows, Fig. 9). Across the tide flats, several acoustically reflective surfaces are observed between 3 and 5 m depth below the modern seafloor, whereas near the base of the delta front these surfaces are more than 20 m below the recently formed sediment wedge. Disruption of the seismic traces by gas is evident also emanating from the shallow subsurface (Fig. 9F, H).

4.4. Sedimentology and stratigraphic change observed in cores

Six sedimentary lithofacies were observed in sediment cores collected along four transects and 40 sediment grabs extending across six transects across the modern emergent marshes, tide flats, and delta front (Fig. 5, Fig. 10): (1) massive sand; (2) cross-bedded sand; (3) silty-sand; (4) mud, (5) laminated mud; and, (6) peat/marsh; the details of these are reported in Grossman et al. (2011). Briefly, the facies were classified based on the sediment grain size, compositional, and textural characteristics. They reflect unique sedimentary environments commonly found in deltaic settings and that may change vertically through a sequence as a result of a change in environment through time or laterally through a deposit where variations or gradients in processes at the same time form different environments (Boggs, 2009).

The massive sand facies were classified based on sediments containing fine to coarse sands and lacking any significant textural properties. The massive sands were common in deeper units of the tide flats and as thin layers or basal units in marsh settings (Fig. 10) with a mean grain size of > 150 μm (Grossman et al., 2011). The cross-bedded sand facies was composed of very fine to medium sands lacking mud with distinct cross-bedding observed in x-radiographs and was very common across the tide flats south of the jetty (Fig. 10), consistent with other recent studies (Webster et al., 2013). The silty-sand facies were characterized by very fine to fine sand with 20–50% silt, mean grain size ranging between 62.5 and 125 μm, and lacking any significant texture. The silty-sand facies occurred in marsh settings and basal sections of several tidal flat and delta front cores (Fig. 10). The mud facies were composed of > 50% silt, a mean sediment grain size < 62.5 μm and massive, lacking texture. The mud facies occurred in marsh and basal sections of the Skagit Bay tidal flat and delta front and dominated surface sediments of the Martha's Bay cores (Fig. 2, Fig. 10A, E). The laminated mud facies contained > 50% silt, had a mean grain size < 62.5 μm and displayed fine horizontal laminae with much greater variability in density and P-wave velocity than other facies and more so with interfingered additional facies. The laminated mud facies occurred in marsh settings and in a several basal sections of tidal flat and delta front cores (Fig. 10B, C, E). The peat/marsh facies largely consisted of organic-rich mud generally containing dense roots and/or marsh peat mats in growth position or detrital root material and was found in the surface units of emergent marsh settings and in a few thin intervals near the base of tidal flat cores (Fig. 10B-E).

4.5. ^{14}C ages and limits on sediment deposit ages

Sediment facies and deposit ages were constrained by ^{14}C dating of wood and carbonate shell materials in addition to the bathymetric change analyses. The wood and carbonate shell materials analyzed were likely not in growth position but instead detrital and therefore include an uncertain amount of time in transport before being deposited (Fig. 10; Table 2). The ^{14}C-derived ages therefore represent maximum constraining ages for the deposits in which they were found, and the

Table 3
Sediment budget and change metrics

(A) Sediment Inputs	Delivery Per Year		Reconstructed Total Input (10^6 m^3)		
	Mass (10^6 kg)	Volume (10^6 m^3)	1890-1939	1940-2014	1890-2014
Total Sediment	2,500	2.94	45.94	69.38	116.25
Sand (density = 1600)	1,500	0.94	98.00	148.00	248.00
Mud (density = 500)	1,000	2.00	143.94	217.38	364.25

(B) Sediment Reservoirs	Volume Accumulated (10^6 m^3)			Reservoir Partitioning (%)		
	1890-1939	1940-2014	1890-2014	1890-1939	1940-2014	1890-2014
Sand	50.15	46.08	96.23			
Delta Front	35.74	28.00	63.73	71.3	60.8	66.2
Fir Island Tide Flats	4.21	12.39	16.59	8.4	26.9	17.2
Martha's Bay Tide Flat	1.89	0.00	1.89	3.8	-	2.0
Other Areas	8.32	5.70	14.02	16.6	12.4	14.6
Mud	19.90	25.41	45.46			
Marshes	7.42	11.20	18.77	37.3	44.1	41.3
Martha's Bay Tide Flat	0.00	5.65	5.65	-	22.2	12.4
Other Areas	12.48	8.55	21.03	62.7	33.7	46.3

(C) Retention	Ratio (Reservoir Volume/Sediment Delivery)			Normalized Retention
	1890-1939	1940-2014	1890-2014	1890–1939
Total Sediment	0.49	0.33	0.39	0.33
Sand	1.09	0.66	0.83	0.74
Mud	0.20	0.17	0.18	0.14
Sand Reservoirs				
Delta Front + Fir Isl. Tide Flats	0.87	0.58	0.69	0.59
Delta Front	0.78	0.40	0.55	0.53
Fir Island Tide Flat	0.09	0.18	0.14	0.06
Martha's Bay Tide Flat	0.04	-	0.02	0.03
Other Areas	0.18	0.08	0.12	0.12
Mud Reservoirs				-
Marshes	0.08	0.08	0.08	0.05
Martha's Bay Tide Flat	-	0.04	0.02	-
Other Areas	0.13	0.06	0.08	0.09

(D) Delta Front Change	Accretion Rate (m/yr)		
	1890-1939	1940-2014	1890-2014
Vertical Accretion Maximum	0.53 ± 0.004	0.36 ± 0.004	
Vertical Accretion Mean	0.08 ± 0.004	0.05 ± 0.004	0.04 ± 0.004
Progradation Maximum	11.33 ± 0.10	5.7 ± 0.07	
Progradation Mean	5.71 ± 0.10	1.67 ± 0.10	3.75 ± 0.05

youngest ages provide the closest approximation for deposit age since they contain the least possible bias for time in transport. The calibrated ages for samples A2-225, C2-140, C5-610, and C6-945 that range 85 ± 56 to 225 ± 56 years have low probabilities of determination and as a result are treated here as modern. The modern to young ^{14}C-derived ages were generally found within the upper 2 m of each core, except samples C5-610, and C6-945 that were found as deep as 6.10 and 9.45 m, respectively. Only two stratigraphic reversals were found and both were located within the diked "reclaimed" area at sites C4 and C6 near historical channels. These are suspected to represent contamination from1800s "reclamation" activities and filling of historical distributary channels or aggradation during the last 100 years resulting from log-jam removals and/or side-cast dredging that eliminated passage of deeper draft steamboat transport through this particular region (Collins, 2000).

5. Discussion

The documented evolution of the study area geomorphology and sedimentary environments since 1890 help to clarify the magnitude of change in sediment delivery and landscape response to western land use. Below we evaluate several components of the Skagit River delta sediment budget and their response to modifications of the sediment regime associated with deforestation, dredging, and channelization. The analyses help to assess their relative contribution to coastal change and their impact relative to long-term Holocene rates of sediment delivery. A case study applying the sediment budget helps to evaluate the region's vulnerability and opportunities to address resilience planning in a coordinated way to serve hazards and ecosystem management goals that will challenge adaptation in the study area and similar settings worldwide.

5.1. Sediment reservoirs and partitioning

5.1.1. Delta progradation constrains fluvial "sand" delivery

The extensive progradation along the entire 14-km long delta front edge and sedimentation of Skagit Bay of up to 25 m since 1890 is consistent with sediment sourced from the Skagit River. The amount of

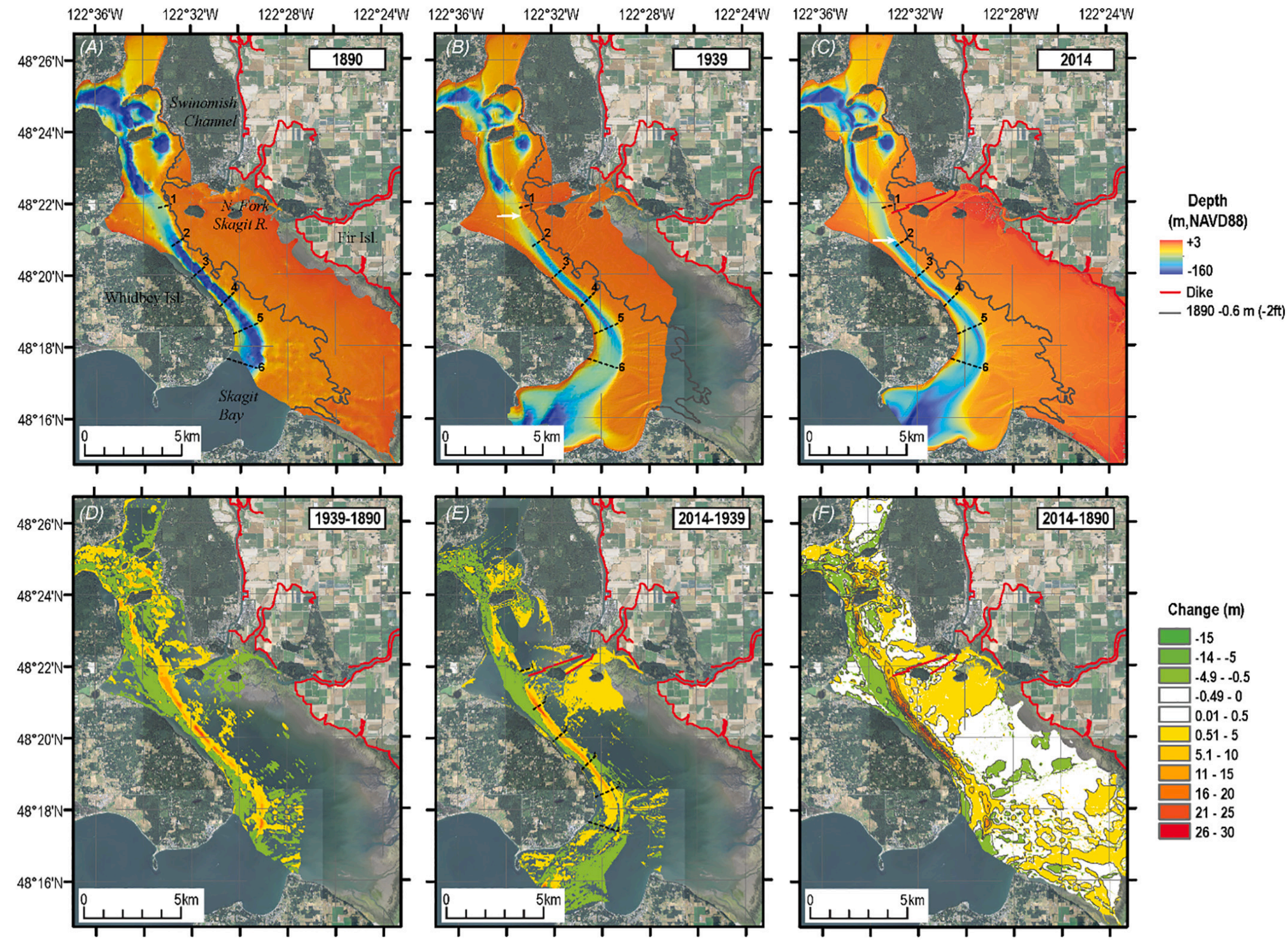

Fig. 6. Map of the bathymetry of the Skagit River delta in 1890 (A), 1939 (B), and 2014 (C) showing up to 750 m of seaward progradation (arrows, 1890 low tide line (-2 ft, 0.6 m) for reference) and significant shallowing of Skagit Bay. Maps showing the difference in bathymetry for the period 1939–1890 (D) 2014–1939 (E) and 2014–1890 (F) reveal the extensive sediment wedge up to 27 m thick that accumulated along the entire 14 km long delta front and areas of accumulation on the tide flats. Transect 1-6 in A-C plotted in Fig. 7.

sand found in the delta front and Fir Island tide flats south of the jetty represent 66 and 17%, respectively, of the total sand accumulated across the study area reflecting the strong retention capacity of these two reservoirs (Table 3). The delta front wedge represented 69–89% of these two reservoirs and shows the extent that sediment bypassed the tide flats and was lost from the emergent delta over this time. The net accumulation of 1–2 m of sediment across the Fir Island tide flats offshore the North and South Forks in bathymetric change (Fig. 6F) and direct evidence of ~ 1 m of sand across the entire tide flats observed in sediment cores (Fig. 10) indicates this reservoir also contains the sand fraction of the river delivery. The stratigraphic correlation of the tide flat cross-bedded sands with the delta front wedge in cores and seismic reflection profiles (Fig. 9) and proliferation of braided channels across the tide flats to the delta edge also suggest a common and large source of fluvial derived sand. Whereas the braided surface texture offshore of the North and South Forks Skagit River reflect the extension of the river distributaries into the bay in part due to the shift in location and number of distributaries (Fig. 2A, B) the relatively uniform thickness and cross-bedding indicates that the surface sands are efficiently redistributed across the entire Fir Island tide flats presumably by waves and tidal currents. At least 1 m of sand across the basal sections of Martha's Bay sediment cores north of the jetty are consistent with sands sourced from the North Fork Skagit River prior to jetty emplacement in 1939 (Fig. 2C, Fig. 5D). Appreciable sedimentation on the order of 5–10 m in other areas surveyed and characterized by relatively high acoustic backscatter intensity (Fig. 8C) are also inferred to be sand or a mix of sand and mud sourced from the Skagit River where local sources are insufficient to account for such accumulation.

5.1.2. Offshore mud accumulation

Reservoirs of mud accumulation since 1890 include the Martha's Bay tide flat, areas surveyed other than the delta front and Fir Island tide flats, and marshes (Fig. 10). Sedimentation across Martha's Bay prior to 1939 remains uncertain as the bathymetric change observed ranging 0.2 to 0.5 m is within stated uncertainty. However, the abrupt facies transition from sand to mud in D1 and D2 sediment cores (Fig. 10A, E) and uniform mud observed across the surface in cores D3-D4 and photographs (Fig. 5D) interpreted to reflect a sudden change from a sandy environment to a mud-dominated depositional environment ca. 1940 when the brunt of the North Fork flow and sand load was redirected by the jetty (Fig. 2C). Cores show the entire area covered on average by 1 m of mud in contrast to other tide flats composed of sand with greater exposure to river discharge and prevailing waves (Crosby and Grossman, 2019). Bathymetric change of 5–20 m in areas surveyed other than the delta front and tide flats characterized by low acoustic backscatter intensity (Fig. 4B, Fig. 8C) are also attributed as mud sourced from the Skagit River and where deeper, calmer settings or areas of complex morphology (Figs. 4A, 8C) and potentially gyre

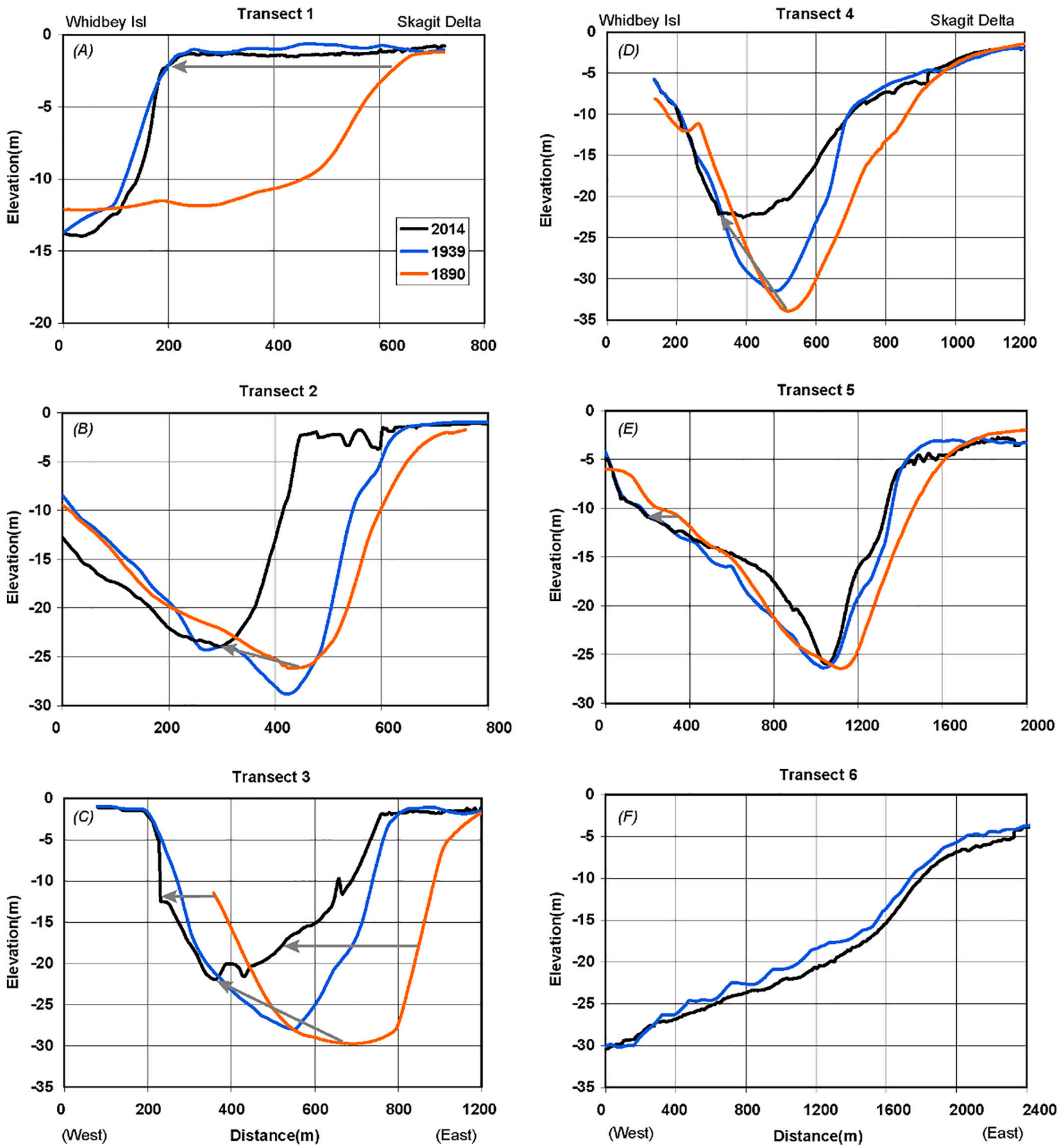

Fig. 7. Line plots of elevation-depth profiles in 1890 (orange), 1939 (blue) and 2010 (black) along six transects in Skagit Bay (locations shown in Fig. 6A-C). More than 400 m of seaward progradation occurred between 1890 and 1939 (grey arrow) directly offshore of the North Fork (A). In the central area of Skagit Bay, tidal flat progradation ranged 200–300 m while the thalweg of Skagit Bay shallowed and moved westward 250–300 m (B, C, D). In southern Skagit Bay, little change has occurred since 1939 (E); 1890 data do not exist for this area. (For interpretation of the references to color in this figure legend, the reader is referred to the web version of this article.)

circulation (Grossman et al., 2020) are conducive for mud deposition. The local watersheds of northern and southern Skagit Bay are argued to be too small to generate sufficient runoff to support such extensive sedimentation and associated accumulation rates of 40–160 mm/yr since 1890 consistent with Webster et al. (2013).

5.1.3. Marsh development and accretion rates

Cores from the hydrologically connected emergent marshes outside the Skagit River delta dike complex show marsh facies comprised of mud and marsh/peat ranging ~1.0–2.0 m thick above sand and silty-sand units (Fig. 10) characteristic of past tidal flat environments (Grossman et al., 2011). The normal grading and increase in organic

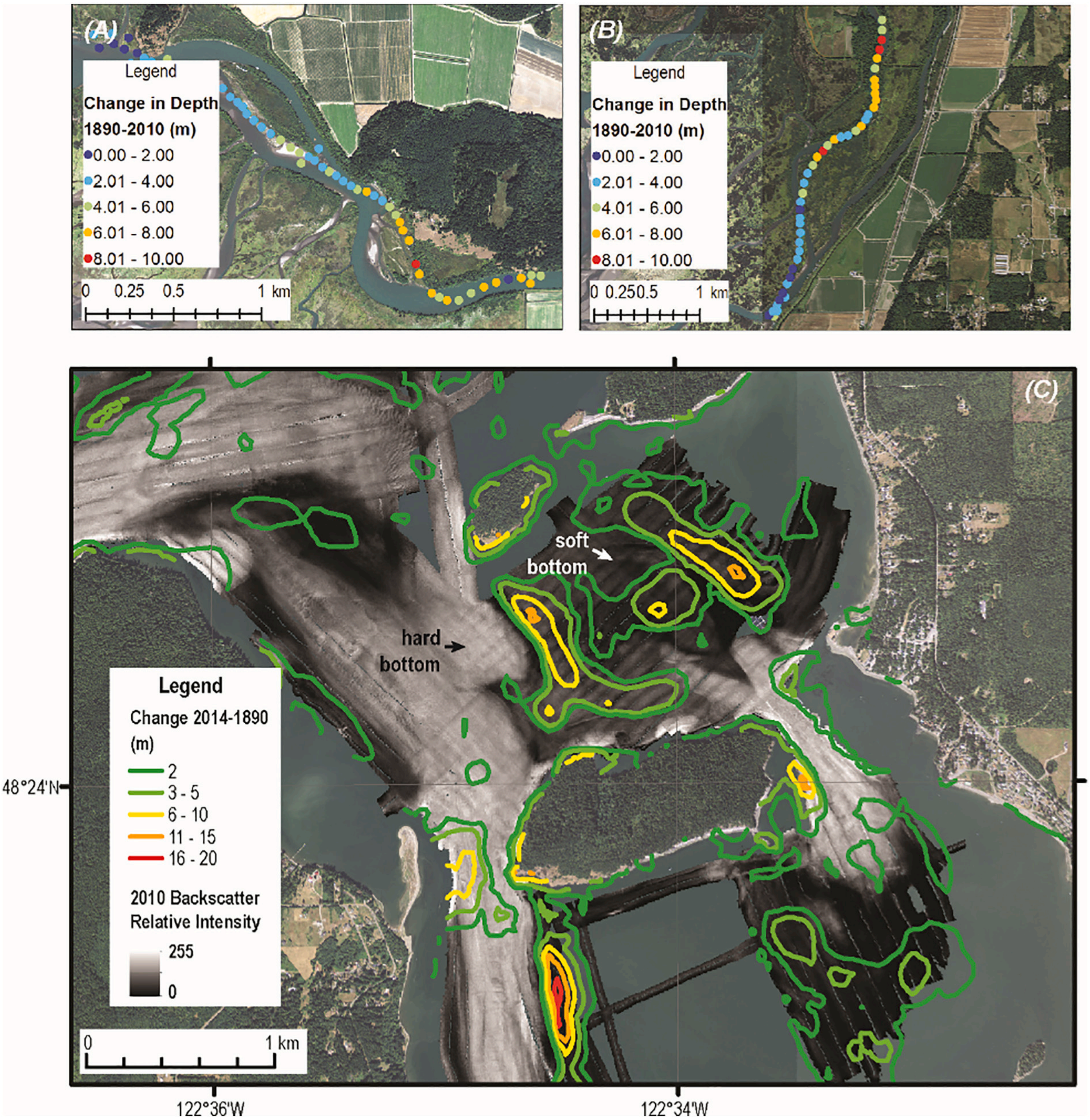

Fig. 8. Maps of bathymetric change in the North Fork (A) and South Fork (B) Skagit Rivers indicate sedimentation assumed to be sand as observed today and in sediment cores (Fig. 10), and other areas surveyed farther from the river mouth showing up to 20 m of sedimentation suspected to be mud associated with low acoustic backscatter intensity (C).

content with elevation in the marsh sediments as represented by core A2 (Fig. 10E) are consistent with recent mud accumulation where muds from the river are transported and settle during tidal exchange. Occasional sand deposits in the marsh facies that range 5–20 cm thick exemplified in core A2 (Fig. 10E) and cores A1, B1, and C1 (Grossman et al., 2011) are thought to result from episodic stream flood events that overtop channel banks and transport significant sand (Curran et al., 2016) and/or coastal storms and waves that resuspend and redistribute tidal flat sands. The mean thickness of the surface mud layer throughout the marsh cores was 1.5 m.

The age of the marsh at site A2 is constrained by modern ^{14}C age and the 1937 photograph, which shows the site in the middle of the North Fork Skagit River channel (Fig. 2C). A derived marsh accretion rate of ~14.2 mm/yr based on this age is likely an upper estimate for the region's marsh complex given its direct and high sediment delivery. Other marsh sites outside the levees, namely A1, B1 and C1, would have maximum accretion rates ranging 6.7–14.3 mm/yr (mean = 8.5 mm/yr) assuming formation over the last 150 years based on their mapped presence in the 1866 GLO cadastral maps. They may be older and therefore be characterized by lower accretion rates. Ages of ^{14}C in cores showed a general stratigraphic continuity, except site C4 and C6 (see below). We estimate ages and accretion rates considering sample C4-914 (age of 472 cal yr BP) to be stratigraphically out of place given the more consistent age relationships observed among samples C4-457, C5-610B, and C5-914 that range 1053 to 2075 cal yr BP with their comparable depths in each core. Marsh accretion rates of 3.3 to 19.4 mm/yr with a mean of 5.6 mm/yr based on ^{14}C-age dating agree closely with the marsh age and accretion relationships based on historical survey, aerial photo, and cored facies thickness data.

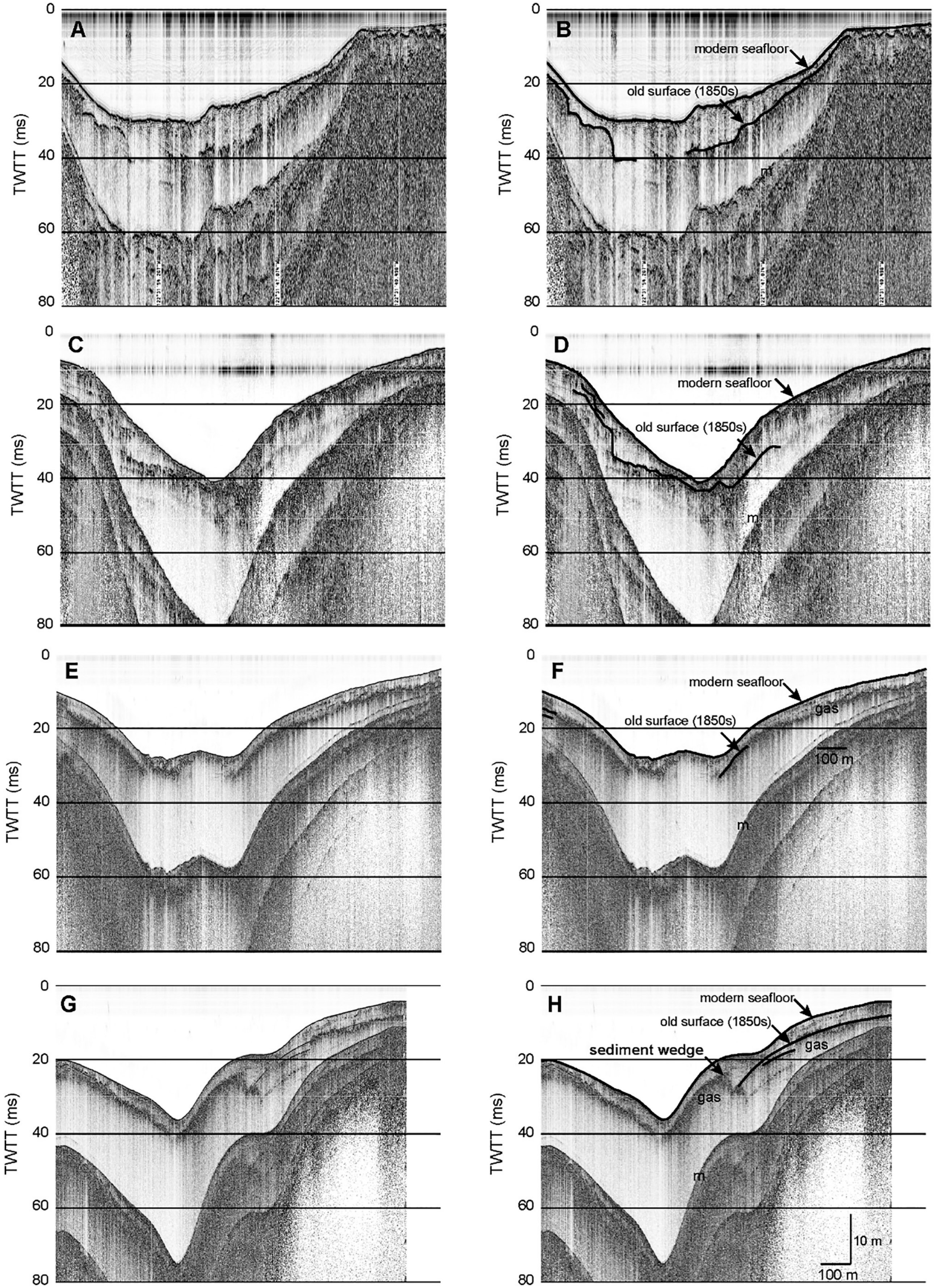

(caption on next page)

Fig. 9. Uninterpreted (left) and interpreted (right) CHIRP seismic-reflection profiles along transects SK1-1 (A,B), SK1-2 (C,D), SK1-3 (E,F), and SK1-4 (G,H) (locations in Fig. 1) showing sediments ranging 5–15 ms (two-way travel time, TWTT) or 3.5–10.5 m in thickness across the outer tide flats conformably drape older buried surface reflectors (arrows) to create the sediment wedge in Figs. 6 and 7. The modern delta front slope is steeper than the older buried surface reflectors. "m" represents a multiple of the seafloor.

5.2. Sediment budget

A total of 142 ± 28 M m^3 of sediment is estimated to have accumulated in the reservoirs surveyed in this study over the period 1890–2014 (Table 3). This amount is comparable to the magnitude and timing of sedimentation in similar coastal systems during this time associated with significant increases in sediment runoff related to activities like deforestation (Nienhuis et al., 2020) and hydraulic mining (Jaffe et al., 2007). The retention of sediment, defined as the amount accumulated relative to delivery, across the Skagit River delta-Bay system represents ~40% of the estimated amount of sediment delivered by the Skagit River applying the suspended sediment load to discharge rating model of (Curran et al., 2016) over the 1940 to 2014 period of observed discharge at USGS stream gage 12200500 (Skagit River at Mount Vernon), and extrapolating the 1940–2014 mean annual load back through 1890. Bedload is also characterized by medium to coarse sand but is not accounted for here representing only 1–3% of the total load (Curran et al., 2016). Estimates of the partitioning of sands and mud among reservoirs and through time by assuming the composition of the Skagit River sediment load of 60% sand and 40% mud (Curran et al., 2016) remained uniform through time are used below to assess potential relative differences in sediment routing in the absence of direct measurements prior to 1970.

5.2.1. Sand

The estimated sand fraction retained in the study area (96 ± 19 M m^3) is equivalent to ~83% of the sand delivered by the river. The total volume change in the delta front of 64 ± 13 M m^3 over the period 1890–2014, is equivalent to 55% of the estimated fluvial delivery of sand by mass (Table 3) based on Curran et al. (2016). Another 17 ± 3 M m^3 of sand is estimated to have accumulated across the Fir Island tide flats between 1890 and 2014 as observed in the upper 1 m of tide flat cores and correlated stratigraphically with the delta front wedge above the 1890 seafloor. It represents 14% of the estimated fluvial delivery of sand by mass (Table 3) and its high retention in these two reservoirs is consistent with its higher density and likelihood to be deposited proximal to the river mouth.

Volume change across other areas of Skagit Bay captured in the bathymetric change analyses and showing high acoustic backscatter (Fig. 9C) represent an additional 15% of the load of sand delivered by the river over this time (Table 3). Another 16% of the estimated sand delivery is unaccounted for in our analyses. Explanations for the missing sand include additional reservoirs like the Skagit River main stem below Mount Vernon (qualitatively shown important here, Fig. 8, but not quantified) and export out of the study area including material that penetrates the Skagit River jetty requiring regular dredging of the Swinomish Channel. Also the bedform asymmetry (e.g., Van Veen, 1935; Stride, 1963) and steep lee sides of 1–3 m tall sand waves at the bottom of Skagit Bay consistently oriented south over repeat bathymetric surveys in 2005, 2007 and 2010 (Fig. 4D, E) suggest sand migration southward and likely out of the study area (Grossman et al., 2018). Additional uncertainty remains regarding the amount that periodically accumulates in the marshes during floods and the extent of change in the fluvial load through time.

5.2.2. Mud

The largest reservoirs of mud accumulation over the period 1890–2014 in our study is within the tidally connected marshes surrounding Fir Island and surveyed areas other than the delta front and Fir Island tide flats. The amount deposited in the marshes totals 19 ± 4 M m^3 and is derived by extrapolating the 1.5 m average thickness of modern marsh facies observed in sediment cores over the 13 m^2 area of marsh (Fig. 2D; Table 3). It represents ~8% of the mud delivery of the Skagit River. Another 6 ± 1 M m^3 of mud can be accounted for covering the Martha's Bay tide flats north and in the protected lee of the Skagit River jetty since 1940 based on findings of our sediment cores (Fig. 6, 10E). This is consistent with net surface tidal-driven and prevailing wind-driven transport (Grossman et al. 2007). Mud deposited there since 1940 represents ~4% of the river mud load since 1940. Mud comprising an assumed 50% of the volume change in other areas captured by the bathymetric change analyses account for ~8% of the river mud delivery since 1890. Approximately 80% of the mud estimated to have been delivered to the bay by the river is unaccounted for and suspected to be largely exported outside of our study area to deeper settings consistent with Webster et al. (2013). Some of the missing mud may also have accumulated along other shoreline and marsh areas north and south of Fir Island, as well as within Fir Island before 1950 and completion of the levee system. Spatially explicit details of historical levee emplacement do not exist.

5.3. Backstrip model reveals extent of land use impact to increase sediment export

The extensive changes noted in progradation and filling of the bay, steepening of the delta front (Figs. 6–9), upward coarsening of facies, abrupt conversion of extensive mud-to sand-dominated tide flat with expansion of braided channel complexes seaward to the outer tide flat edge (Fig. 1, Fig. 2D, Fig. 6E) are consistent with an increase in sediment supply. The greatest progradation and vertical accumulation of sediment in the north-central area between transects 1 and 3 (Fig. 7) and general decrease southward are consistent with a greater portion of the Skagit River sediment load routed through the North Fork, particularly during high flows (Curran et al., 2016). The steepening of delta front slopes along the north-central transects from 1890 to 2014 implies an increase in sediment flux, particle size, and/or change in hydrodynamics offshore to support the steeper gradients (Fig. 7, Fig. 8). These changes and correlative sand facies observed in tide flat cores (Fig. 10) support the notion that the progradation and vertical filling of the bay was accommodated particularly by an increase in the delivery of sand to the bay.

Comparison of the extensive volume expansion and progradation observed to potential past rates of change indicate that the rate of sediment delivery offshore of the emergent delta due to land use since 1890 was significantly greater than the long-term average Holocene rate. This is derived by employing a geomorphic backstripping approach (Kang and Xie, 2013; Zhao et al., 2013) that reconstructs the past landscape through sequential unstacking or removal of morphology and testing the consistency between or plausibility of observed, modeled or assumed factors like sedimentation rate to explain morphologic change thorough time. Applying the change rates observed (Figs. 6, 7, Table 3) and stripping away the delta front, tidal flat, and bay morphology formed since 1890 ((.ure 11A), back in time would imply the delta front migrated ~6–7 km from a location near the present shoreline in ~8 steps equivalent to 1,022 years (Fig. 11B). This model of change implies excessively high sediment delivery that would have transformed a deep 20–30 m bay extending immediately offshore of the 1,022 year old shoreline to Whidbey Island into the shallow 51 km^2 tidal flat area observed today. This is inconsistent with the 1890 and 1939 historical bathymetry, shallow seismic reflection profile data (Fig. 9), and ^{14}C age supported stratigraphy showing a gently sloping

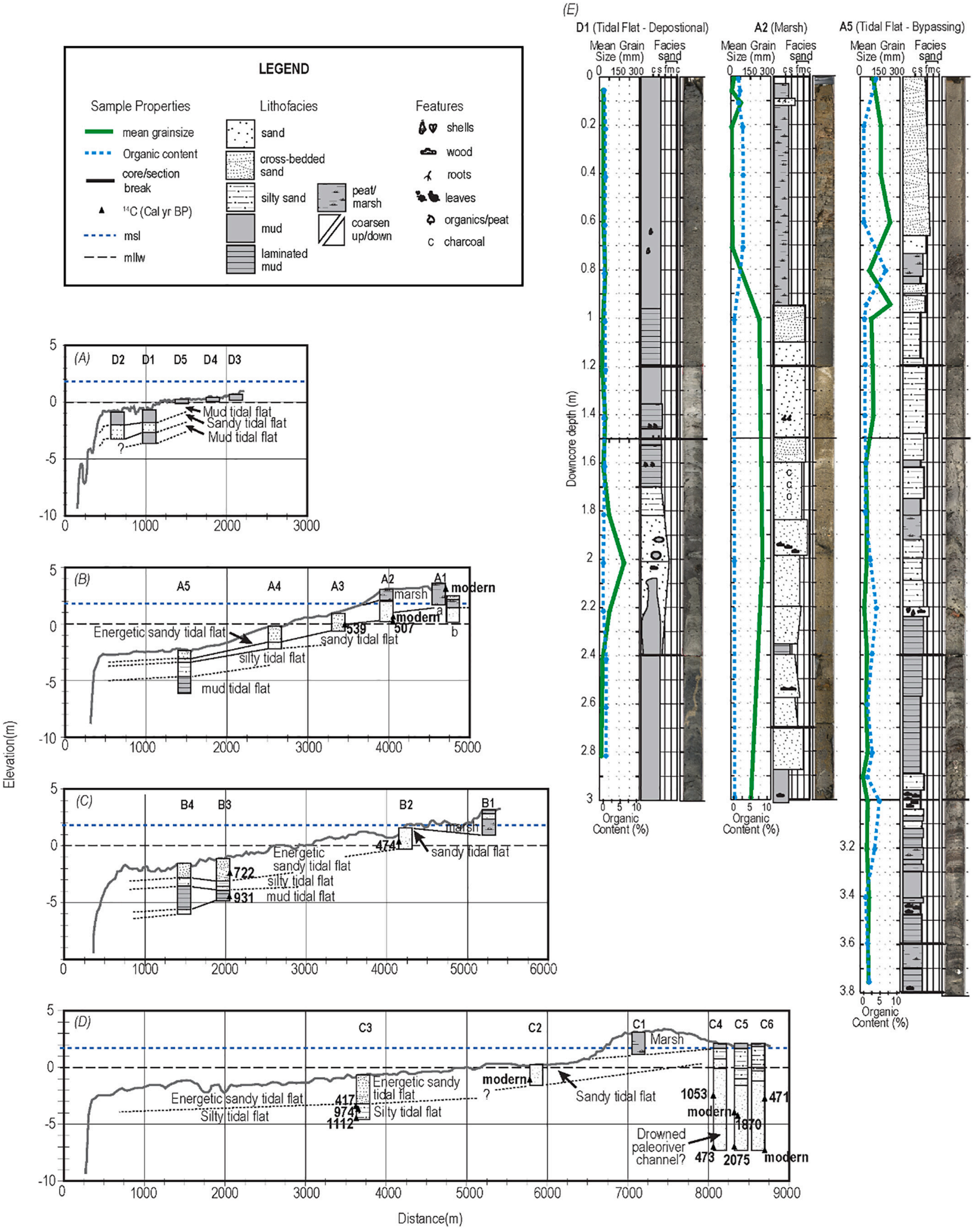

Fig. 10. Diagram showing stratigraphic relationships along core transects (A-D), and facies information and photographs observed from sediment cores (E) showing the distinctly finer surface mud layer of the Martha's Bay tide flat (core D1), representative marsh facies above older sand flat units (core A2), and cross-bedded sand over buried laminated mud units characteristic of the outer Fir Island tide flats (core A5).

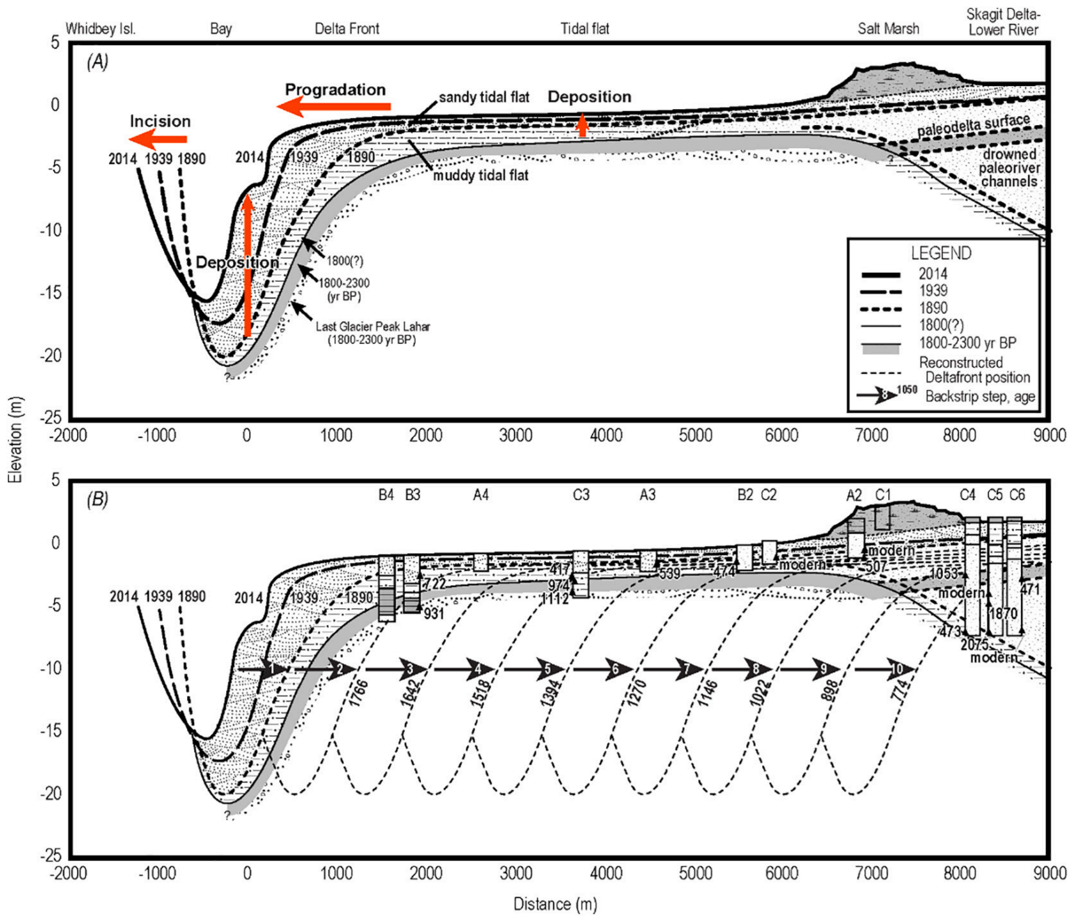

Fig. 11. Diagrams showing the stratigraphic evolution of the Skagit River delta since 1890 (A) and geomorphic backstripping reconstruction of past delta morphology (B) showing that the observed sediment delivery rate between 1890 and 2014 over predicts the Holocene rate as reconstructed morphology in 124 years steps (arrows) is inconsistent with and removes structure and lithology interpreted from bathymetry, seismic reflection profiling, sediment cores (this study), and other studies (Dragovich et al., 2000) within just a few hundred years.

older delta surface and subsurface architecture ranging 400–1000 yr BP within 1–10 m of the tidal flat and marsh surface (Fig. 10; Table 2). A more plausible explanation for the extensive delta progradation, abrupt coarsening in sediment textures (laminated to cross bedding in core samples), and steepening of the delta front observed is a 10-fold increase in sediment flux beginning with initial logging followed by dredging and channelization activities. An order of magnitude increase is consistent with and helps explain a marked change in shoreline progradation rate from ~2 m/yr over the last 5000 years ago based on archaeology (Dragovich et al., 2000) to ~20 m/yr since the 1850s (Hood et al., 2016). Even compensating for a doubling of sediment compaction which is significantly higher than observed in any cores (Grossman et al., 2011) would necessitate a 5-fold increase in sediment flux the last 120 years.

5.4. Sediment retention and morphology inform relative contributions of logging and channelization to sediment export

Variations in delta morphology, facies composition, and sediment accumulation since 1890 help evaluate in the influences of land uses to sediment delivery since the 1890s. Normalizing the amount of sand accumulated in the delta front wedge during the periods 1890–1939 (36 M m^3) and 1940–2014 (28 M m^3), by the mean annual fluvial input of sand based on Curran et al. (2016), suggests that sand flux offshore to the delta front was nearly twice as high in the early period (Table 3). The higher sand retention of the delta front before 1939 (0.78) relative to after 1940 (0.40) is consistent with a greater rate of sand delivery prior to 1940. Peak and mean vertical accumulation rates of the delta front during the 1890–1939 period of 53.12 ± 0.36 and 8.22 ± 0.36 cm/yr, respectively, were also higher than those of the 1940–2014 period (peak, 35.95 ± 0.35 cm/yr; mean, 5.07 ± 0.35 cm/yr). Along with higher maximum (11.33 ± 0.10 m/yr) progradation rates in the 1890–1939 period than 1940–2014 period (5.70 ± 0.07 m/yr) these changes in sedimentation patterns are consistent with greater sediment delivery are interpreted here related at least in part to the influence of late 1800s and early 1900s deforestation that led to a near complete denudation of the Puget Sound landscape and large wood removal and dredging activities in the main-stem river channel (Collins, 2000). A shift to overall lower delta front retention and sedimentation after 1940 is also conversely related to improved forest practices following 1940. Recent studies indicate that sediment transport of significant fractions of fine materials sourced from debris flows reach the shoreline in hours to days (Tucker et al., 2014; Nowacki and Grossman, 2020).

Interestingly, the lower accumulation and sediment retention in the delta front after 1940 was also associated with higher retention of sand across the Fir Island tide flats after 1940 (0.18) than before (0.09) (Table 3). At face value, if we assume the 32% decrease in total sediment retention after 1940 resulted from the reduced impacts of early deforestation and improved forest management practices, the higher delivery rate of sand to the tide flats after 1940 supports the argument that river channelization continued to efficiently focus sediment offshore. We further explore the potential magnitude related to these land use activities by normalizing the 1890–1939 reservoir retention estimates by 68%, equivalent to the decrease in total sediment retention from 0.49–0.33 after 1940 (Table 3). Prior to normalizing, the delta front experienced a 48% decrease in sand retention after 1940 whereas removing these assumed affects normalizing by 68% cut that decrease to 25%, suggesting that early land uses contributed to at least half of the change observed after 1940. Across the Fir Island tide flats sand retention without normalizing increased by ~100% (two-fold) after 1940. Normalizing and removing the assumed effects of deforestation, snagging and dredging prior to 1940, suggests that other influences led to a 3-fold increase in the retention of sand over the Fir Island tide flats after 1940. It is likely that higher retention over the Fir Island tide flats was in part a positive feedback response to the rapidly prograded delta and substrate coarsening that would impart higher friction and attenuation. Comparable retention of the delta front and other offshore reservoirs over time however indicate that additional factors contributing to the higher export in the system relative to the past, the principal one after 1940 being channelization, continue to operate and drive significant sediment bypassing and loss from the emergent delta.

5.5. Impacts of and opportunities to recover lost sediment resources

Several direct impacts of the increased flux of sediment offshore away from the emergent delta are observed and related to natural hazards risk management, agricultural resilience planning, and habitat and ecosystem recovery goals. A brief description of these impacts and a case study demonstrating the application of the sediment budget is discussed as an example for evaluating opportunities to enhance resilience and planning, pertinent to many coastal and delta systems.

5.5.1. Hazards associated with accelerated delta progradation

The rapid extension of the delta seaward, delta front steepening, sedimentation of Skagit Bay, and reduced supply of sediment to coastal areas including valued agricultural lands experiencing subsidence have important implications for and likely exacerbate natural hazards risk and flood management. The rapid buildup of up to 10–20 m of unconsolidated sands along the delta front has led to an increase in delta front slope offshore of the North Fork Skagit River (Fig. 12A-C). The structural stability and potential for failure of these steep, unconsolidated deposits remain uncertain but are a concern given the region's active tectonics (Barnhardt and Sherrod, 2006). Similar historical deposits and many that are much steeper characterize other river-delta systems where channelization has occurred worldwide in addition to the Pacific Northwest.

In response to the 300–500 m migration of the delta and bay to the west, more than 200–300 m of erosion of the submerged flanks of Whidbey Island has occurred (Figure 7). The extent that erosion along the Whidbey Island shoreline has occurred or is influenced by the incision documented is unknown and outside the scope of this study. Several transects studied however, revealed uniform rates of change through time, whereas Transect 2 and a portion of Transect 3 showed more rapid incision between 1940 and 2014 than prior to 1939 (Fig. 7). A finer spatial assessment of these changes and the underlying geologic framework of the submerged flanks of Whidbey Islands may be important to inform potential pending shoreline change as erosion upslope toward the beaches and bluffs. Eventual erosion of the eastern Whidbey Island shore exacerbated by the high Skagit River sediment export and westward progradation of the delta is likely given the 25% reduction in flow conveyance of the north-central Skagit Bay observed since 1890 (Fig. 12D, location in Fig. 4A). The reduction in flow conveyance focused on the volume of the bay below the tide flat-delta front slope break where flow is most constrained. It is likely to experience increases in flow velocities as additional bay sedimentation occurs with expected increases in fluvial sediment runoff projected as a result of more intense rainfall and a greater percentage of precipitation as rain than snow as the Pacific Northwest warms (Lee et al., 2016). It remains unclear if the reduction in flow conveyance has impacted the region's ecology through mixing and transport important to processes like the transport of larvae or dispersal of nutrients.

5.5.2. Impacts of sediment export to habitats and ecosystem services

The extensive change from a mud-rich tidal flat to a more energetic, sand-dominated environment of braided channel complexes across the expansive tide flats offshore of Fir Island represents a wholesale transformation in habitat and ecosystem structure. A poorly understood concern of the effects of levees and dikes (Hood, 2004) is the extent that high flux of coarse sediment and chronic abrasion, burial and/or scour fragments or impairs habitats offshore. Such disturbances commonly lead to lower biodiversity and biomass, disconnected habitats, and impaired water quality including light reduction by finer material in suspension (Ysebaert and Herman, 2002; Ysebaert et al., 2003; van der wal et al., 2017). Important habitat in the form of seagrass meadows offshore of the North and South Forks that continue to be fragmented by the high sediment flux bypassing the tide flats have been shown to be important to juvenile Chinook salmon (Rubin et al., 2018), many other estuarine wildlife (Toft et al., 2018), and are a principal focus for salmon recovery. The exported sediment is an important resource to maintain marshes which also serve as essential juvenile rearing habitat for several salmon species (Beamer et al., 2005). Recent findings of marsh loss along the central Fir Island shoreline (Hood et al., 2016), despite being fed by the highest fluvial sediment load in Puget Sound (Czuba et al., 2011), reveal the complexity of and need for improved understanding of sediment budgets and routing and coordinated efforts to minimize sediment impacts to ecosystem services people depend on.

5.5.3. Opportunities to recover sediment for enhancing resilience

The derived sediment budget and improved understanding of the fraction lost offshore provides important quantitative information to assess and identify potential solutions for enhancing resilience. Relative subsidence across Fir Island, the Skagit River lowlands, and similar coastal areas worldwide where the emplacement of levees have eliminated sediment delivery is leading to greater vulnerability to sea-level rise and flooding from rivers and groundwater. In addition to lost sediment replenishment with river floods, these areas often experience compaction associated with land use and commonly sedimentation outside the levee network that impedes drainage. Analyses of the 2014 elevation data show that ~70% of Fir Island lies below mean higher high water where the average monthly highest tide reaches (Fig. 12E). Surface elevations range up to 5.2 m below MHHW (in channels) with the average elevation 0.6 m below MHHW and an associated volume of space equal to 13 M m^3 below the monthly high tide line. Over the past 124 years, this entire area would have maintained its grade and natural ability to mitigate floods up to MHHW with a mere ~5% of the annual sediment load of the Skagit River deposited across Fir Island (blue curve, Fig. 12F). Looking forward into the future, given the present sediment load, it could take up to 22 years diverting 20% of the fluvial sediment load to rebuild the elevation of Fir Island sufficiently to mitigate flooding impacts across the subsided area (red curve, Fig. 12F). Whereas this example clarifies potential opportunities to enhance resilience, it likely underestimates the total risk associated with uncertainties of future sediment delivery, sea-level rise, and land use but elucidates the gravity of the challenges coastal communities face. Here, as in many similar systems, our geomorphic analysis indicates the potential redistribution of sediment currently lost offshore to the emergent delta could have mutual benefits to diverse concerns including natural-hazards risk management, fisheries, agriculture, and general adaptive planning for expected population growth and climate-change impacts throughout the region.

6. Conclusions

Natural hazard risk and ecosystem management in coastal and deltaic environments is limited by poor understanding of sediment budgets and transport dynamics. In this study, analyses of bathymetric

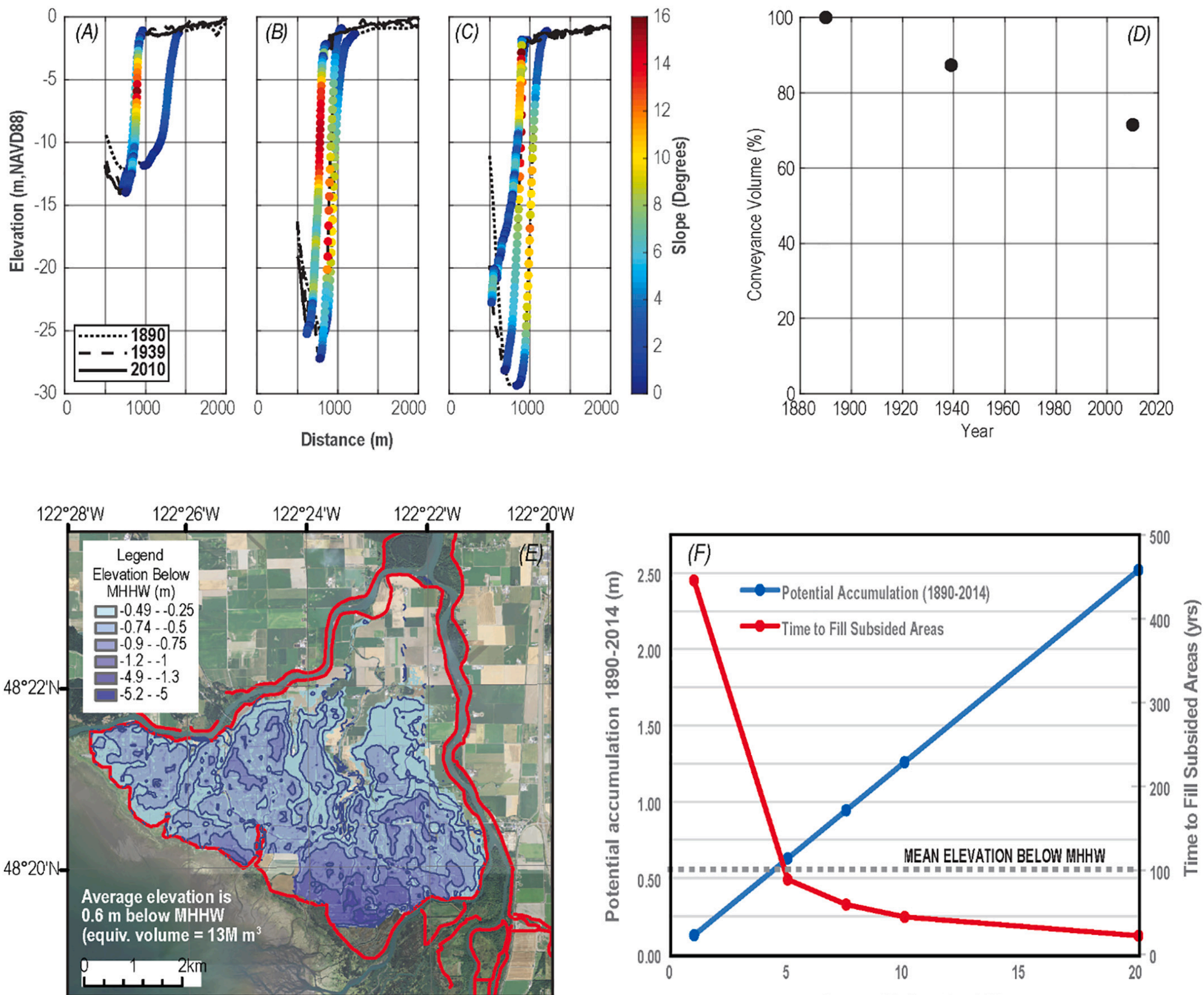

Fig. 12. Diagrams showing impacts of sediment export. (A-C) Plots showing the rapid steeping the delta front over time across transects 1-3 (Fig. 7) with unconsolidated sands vulnerable to failure. (D) Plot of the change in flow conveyance of central Skagit Bay in response to the delta progradation since 1890 (location in Fig. 4) showing a 22% reduction in the volume capacity for circulation and mixing. (E) Map showing the distribution of land surface elevations of Fir Island in 2014 ranging 0 to 5.2 m below Mean Higher High Water (mean = 0.6 m) associated with lost sediment supply and subsidence. (F) Plot of the potential vertical sediment accumulation over Fir Island that could have been gained between 1890 and 2014 (blue line) and the time in years in the future (red line) required to fill the equivalent volume of 13M m^3 associated with area 0.6 m below MHHW assuming up to 20% of the Skagit River sediment delivery to Fir Island. (For interpretation of the references to color in this figure legend, the reader is referred to the web version of this article.)

change, sediment cores, and modeling were used to show how an estimated 142 ± 28 M m^3 of sediment accumulated across the large Skagit River delta between 1890 and 2014 relates to land uses. The amount stored in the reservoirs analyzed represents ~39% of the total estimated delivery over this time, however accumulation of 83% of the fluvial sand fraction found near the river mouth make retention in the delta foreset and tide flats effective metrics to evaluate land use impacts on sediment dynamics and ecosystems through time. A significantly higher ratio of sand retention during the period 1890–1939, coinciding with extensive deforestation, channel dredging, and channelization activities, was found relative to the period 1940–2014, which was characterized by improved forest practices and sediment management to protect endangered species. The retention ratio of sand accumulated relative to delivered greater than one also indicates that sand supply was significantly higher during the period 1890–1939 than present. Sand retention offshore was comparable over time but significantly higher across the extensive tide flat subsequent to 1940. Normalizing for the assumed effects of improved forest practices (e.g., reduced sediment runoff) suggests that channelization has continued to influence sediment export at a magnitude equivalent to the effects of earlier logging. The majority (87%) of the sediment accounted for in this study accumulated offshore of the emergent delta, reflecting the extent that western land use abruptly and efficiently rerouted sediment offshore. The resulting flux of sediment offshore and bypassing of the emergent delta represents a 5–10x increase over Holocene rates.

The extent that higher flux through the coastal zone per unit area associated with western land use has adversely impacted valued ecosystem services, and regional resilience has remained poorly quantified. This study, however, has shown that the abrupt and significant increase in sediment export transformed the expansive Skagit River delta tide flats from a calmer depositional environment dominated by mud, known to support greater biodiversity, to a more energetic fluvial dominated environment characterized by chronic sediment disturbance, habitat abrasion, burial, and fragmentation. The increase in flux of coarser sediment offshore has also led to sufficient delta progradation and sedimentation across the offshore embayment to: (1) reduce the fjordal-bay's flow conveyance 28%, (2) induce erosion of the neighboring Whidbey Island as the bay circulation migrated westward, and (3) steepen the delta front with unconsolidated sands vulnerable to failure if perturbed by the region's active tectonics. The sediment transported offshore represents a lost resource for the emergent delta facing increasing vulnerability to sea level rise. Despite the highest sediment load of all Puget Sound rivers, the sediment export offshore helps to explain recent widespread erosion of Skagit Bay coastal marshes.

The sediment budget and historical change analyses reported here provide a framework to assess coastal responses to sediment delivery and routing to guide vulnerability assessments and resilience planning. The quantitative measures of exported sediment inform opportunities to address vulnerabilities, including recovering subsiding farmland that lost the sediment resource due to channelization and are important to the world's vegetable production. The sediment budget analysis here indicates that redirecting and retaining up to just 20% of the river sediment load within the emergent delta could significantly raise the grade to compensate for the subsidence experienced since the levees were emplaced. More than 22 years appears to be required at this 20% recovery rate to establish elevations that can be naturally maintained and able to mitigate monthly extreme tidal flooding. Whereas coastal vulnerability assessments have considered projected changes in sea level and sediment availability, sediment budget and coastal change assessment helps elucidate the extent that land uses continue to and may further exacerbate their impacts to multiple, interrelated sectors of society important to trade-off decisions facing floodplain and ecosystem management strategies and long-term resilience planning.

Declaration of Competing Interest

None

Acknowledgements

We thank Greg Hood and Skagit River System Cooperative, Martin Sampson, Todd Mitchell, Sarah Grossman and Swinomish Indian Tribal Community, Doug Bulthius and Padilla Bay National Estuarine Research Reserve, and Renee Takesue, Guy Gelfenbaum, and Brad Carkin and USGS Pacific Coastal and Marine Science Center Marine Facility for extensive field and laboratory support. We acknowledge the efforts of Steward Fallon (CAMS, now ANU) for assistance analyzing sediment ages with ^{14}C. We thank Patrick Barnard and anonymous reviewers for their thorough critique of this manuscript. Funding for this study was provided by the U.S. Geological Survey Coastal and Marine Hazards and Resources Program as part of the Coastal Habitats in Puget Sound Project and the Office of Naval Research Coastal Geosciences Program. Any use of trade, firm, or product names is for descriptive purposes only and does not imply endorsement by the U.S. Government.

References

Kang, Bo, Xie, Xinong, 2013. Geomorphology backstripping: a numerical approach for quantitatively reconstructing the paleo-geomorphology in passive margins and deltaic basins. pp. 1826–1832. https://doi.org/10.1190/segam2013-0576.1.

Paulson, K., 1997. Estimating changes in sediment supply due to forest practices: A sediment budget approach applied to the Skagit River Basin in Northwestern Washington. University of Washington Masters Thesis.

Anthony, E.J., Marriner, N., Morhange, C., 2014. Human influence and the changing geomorphology of Mediterranean deltas and coasts over the last 6000 years: From progradation to destruction phase? Earth Sci. Rev. 139, 336–361. https://doi.org/10.1016/j.earscirev.2014.10.003.

Barnhardt, W.A., Sherrod, B.L., 2006. Evolution of a Holocene delta driven by episodic sediment delivery and coseismic deformation, Puget Sound, Washington, USA. Sedimentology 53 (6), 1211–1228.

Barnosky, A.D., Hadly, E.A., Bascompte, J., Berlow, E.L., Brown, J.H., Fortelius, M., Getz, W.M., Harte, J., Hastings, A., Marquet, P.A., Martinez, N.D., Mooers, A., Roopnarine, P., Vermeij, G., Williams, J.W., Gillespie, R., Kitzes, J., Marshall, C., Matzke, N., ... Smith, A.B., 2012. Approaching a state shift in Earth's biosphere. Nature 486 (7401), 52–58. https://doi.org/10.1038/nature11018.

Beamer, E., Bernard, R., Hayman, B., Hebner, B., Hinton, S., Hood, G., Kraemer, C., McBride, A., Musslewhite, J., Smith, D., Wasserman, L., Wyman, K., 2005. Skagit Chinook recovery plan. http://www.skagitcoop.org/.

Boggs, S., 2009. Principles of Sedimentology and Stratigraphy (5th Ed). Pearson Prentice Hall, Upper Saddle River, N.J, pp. 688.

Booth, D.B., 1994. Glaciofluvial infilling and scour of the Puget Lowland, Washington, during ice-sheet glaciation. Geology 22 (8), 695–698.

Bortleson, G.C., Chrzastowski, M.J., Helgerson, A.K., 1980. Historical changes of shoreline and wetland at eleven major deltas in the Puget Sound region. U.S. Geological Survey Hydrologic Investigations Atlas HA-617, Washington 11 sheets.

Cardinale, B.J., Duffy, J.E., Gonzalez, A., Hooper, D.U., Perrings, C., Venail, P., Narwani, A., MacE, G.M., Tilman, D., Wardle, D.A., Kinzig, A., Daily, G.C., Loreau, M., Grace, J.B., Larigauderie, A., Srivastava, D.S., Naeem, S., 2012. Biodiversity loss and its impact on humanity. Nature 486 (7401), 59–67. https://doi.org/10.1038/nature11148.

Chu, Z.X., Zhai, S.K., Lu, X.X., Liu, J.P., Xu, J.X., Xu, K.H., 2009. A quantitative assessment of human impacts on decrease in sediment flux from major Chinese rivers entering the western Pacific Ocean. Geophys. Res. Lett. 36 (19), 1–5. https://doi.org/10.1029/2009GL039513.

Collins, B., 1998. Preliminary assessment of historic conditions of the Skagit River in the Fir Island area: Implications for Salmonid Habitat restoration. Report to Skagit System Cooperative, pp. 72.

Collins, B., 2000. Mid-19th century stream channels and wetlands interpreted from archival sources for three north Puget Sound estuaries, Prepared for Skagit System Cooperative, Bullitt Foundation. Skagit Watershed Council. University of Washington, Seattle, WA, pp. 65.

Crosby, S.C., Grossman, E.E., 2019. Wave observations from nearshore bottom-mounted pressure sensors in Skagit and Bellingham Bays, Washington, USA from Dec 2017 to Feb 2018. U.S. Geological Survey data releasehttps://doi.org/10.5066/P9JZ5F00.

Curran, C., Grossman, E.E., Mastin, M., Huffman, R., 2016. Sediment Load and Distribution in the Lower Skagit River, Skagit County, Washington. USGS Scientific Investigations Report, pp. 25 2016-5106.

Czuba, J.A., Magirl, C.S., Czuba, C.R., Grossman, E.E., Curran, C.A., Gendaszek, A.S., Dinicola, R.S., 2011. Sediment load from major rivers into Puget Sound and its adjacent waters. U.S. Geological Survey Fact Sheet 2011–3083, pp. 4. http://pubs.usgs.gov/fs/2011/3083/.

Dragovich, J.D., McKay, D.T., Dethier, D.P., Beget, J.E., 2000. Holocene Glacier Peak Lahar Deposits in the Lower Skagit River Valley, Washington. Wash. Geol. 28 (1/2), 19–21.

Gaeckle, J.L., Dowty, P., Berry, H., Ferrier, L., 2009. Puget Sound Submerged Vegetation Monitoring Project: 2008 Monitoring Report, Nearshore Habitat Program. Washington State Department of Natural Resources, Olympia, WA.

Ganju, N.K., Define, Z., Kirwan, M.L., Fagherazzi, S., D'Alpaos, A.D., Carniello, L., 2017. Spatially integrative metrics reveal hidden vulnerability of microtidal salt marshes. Nat. Commun. 8 (14156), 1–7.

Goisan, L., Constantinescu, S., Filip, F., Deng, B., 2013. Maintenance of large deltas through channelization: Nature vs. humans in the Danube delta. Anthropocene 1, 35–45.

Grossman, E.E., Stevens, A., Gelfenbaum, G., Curran, C., 2007. Nearshore circulation and water column properties in the Skagit River Delta, northern Puget Sound, Washington—Juvenile Chinook salmon habitat availability in the Swinomish Channel. U.S. Geological Survey Scientific Investigations Report 2007–5120, pp. 96. http://pubs.usgs.gov/sir/2007/5120/.

Grossman, E.E., George, D.A., Lam, A., 2011. Shallow stratigraphy of the Skagit River Delta, Washington, USA derived from sediment cores. USGS Open-File Report 2011-1194.

Grossman, E.E., Dartnell, P., Finlayson, D.P., 2018. High-resolution bathymetry and acoustic-backscatter data collected in 2004, 2005, 2007, and 2010 in Skagit Bay. U.S. Geological Survey data release, Washington. https://doi.org/10.5066/F7JM27VN.

Grossman, S.K., Grossman, E.E., Barber, J.S., Gamblewood, S.K., Crosby, S.C., 2020. Distribution and transport of Olympia oyster, Ostrea lurida, larvae in Northern Puget Sound, Washington, USA. J. Shellfish Res. 39 (2), 215–233. https://doi.org/10.2983/035.039.0204.

Hood, W.G., 2004. Indirect environmental effects of dikes on estuarine tidal channels: thinking outside of the dike for habitat restoration and monitoring. Estuaries 27 (2), 273–282.

Hood, W.G., Grossman, E.E., Veldhuisen, C., 2016. Assessing tidal marsh vulnerability to sea-level rise in the Skagit River Delta. Northwest Science. 90 (1), 79–93.

Jackson, D.R., Briggs, K.B., Williams, K.L., Richardson, M.D., 1996. Tests of models for high-frequency seafloor backscatter. IEEE J. Ocean. Eng. 21 (4), 458–470.

Jaeger, K.L., Curran, C.A., Anderson, S.W., Morris, S.T., Moran, P.W., Reams, K.A., 2017. Suspended sediment, turbidity, and stream water temperature in the Sauk River Basin, Washington, water years 2012–16. US Geol. Surv. Sci. Investig, pp. 47. https://doi.org/10.3133/sir2017511. Rep. 2017–5113.

Jaffe, B.E., Smith, R.E., Foxgrover, A.C., 2007. Anthropogenic influence on sedimentation and intertidal mudflat change in San Pablo Bay, California: 1856-1983. Estuar. Coast. Shelf Sci. 73, 175–187.

Kirwan, M.L., Megonigal, J.P., 2013. Tidal wetland stability in the face of human impacts and sea-level rise. Nature 504, 53–60.

Lee, Se-Yeun, Hamlet, A.F., Grossman, E., 2016. Impacts of Climate Change on Flood Control, Hydropower Production, Regulated Low Flows, and Sediment Discharge in the Skagit River Basin. Northwest Science. 90 (1), 23–43.

Lotze, H.K., Lenihan, H.S., Bourque, B.J., Bradbury, R.H., Cooke, R.G., Kay, M.C., Kidwell, S.M., Kirby, M.X., Peterson, C.H., Jackson, J.B., 2006. Depletion, degradation, and recovery potential of estuaries and coastal seas. Science 312, 1806–1809.

McBride, A., Wolf, K., Beamer, E.M., 2006. Skagit Bay nearshore habitat mapping. Skagit River System Cooperative. http://www.skagitcoop.org/documents/EB2180_McBride%20et%20al_2006.pdf.

Miller, I.M., Yang, Z., VanArendonk, N., Grossman, E., Mauger, G.S., Morgan, H., 2019. Extreme Coastal Water Level in Washington State: Guidelines to Support Sea Level Rise Planning. In: A collaboration of Washington Sea Grant, University of Washington Climate Impacts Group, Oregon State University, University of Washington, Pacific Northwest National Laboratory and U.S. Geological Survey. Prepared for the Washington Coastal Resilience Project.

Moftakhari, H.R., Jay, D.A., Talke, S., Schoellhamer, D.H., 2015. Estimation of historic flows and sediment loads to San Francisco Bay, 1849–2011. J. Hydrol. 529 (Part 3), 1247–1261.

Nesbit, D.M., with Contributions from U. S. Coast Survey, S. L. Boardman, Eldridge Morse, and others, 1885. Tide marshes of the United States. USDA Miscellaneous Special Report No. 7. Government Printing Office, Washington, D. C.

Nicholls, R.J., Cazenave, A., 2010. Sea-Level Rise and Its Impact on Coastal Zones. Science 328 (5985), 1517–1520.

Nienhuis, J.H., Ashton, A.D., Edmonds, D.A., et al., 2020. Global-scale human impact on delta morphology has led to net land area gain. Nature 577, 514–518. https://doi.org/10.1038/s41586-019-1905-9.

Nowacki, D.J., Grossman, E.E., 2020. Sediment transport in a restored, river-influenced Pacific Northwest estuary. Estuarine Coastal Shelf Sci. 242, 10. https://doi.org/10.1016/j.ecss.2020.106869.

Ralston, D.K., Geyer, W.R., Traykovski, P.A., Nidzieko, N.J., 2013. Effects of estuarine and fluvial processes on sediment transport over deltaic tidal flats. Continental Shelf Res. 60S, 40–57.

Rubin, S.P., Hayes, M., Grossman, E.E., 2018. Juvenile Chinook salmon and forage fish use of delta eelgrass influenced by diking and river channelization. Marine and Coastal Fisheries, pp. 58.

Stanley, D.J., Warne, A.G., 1994. Worldwide initiation of Holocene marine deltas by deceleration of sea-level rise. Science 265, 228–231.

Steffen, W., Richardson, K., Rockström, J., Cornell, S.E., Fetzer, I., Bennett, E.M., Biggs, R., Carpenter, S.R., de Vries, W., de Wit, C.A., Folke, C., Gerten, D., Heinke, J., Mace, G.M., Persson, L.M., Ramanathan, V., Reyers, B., Sörlin, S., 2015. Planetary boundaries: Guiding human development on a changing planet. Science 347, 1–10.

Stevens, A.W., Lacy, J.R., Finlayson, D.P., Gelfenbaum, G., 2008. Evaluation of a single-beam sonar system to map seagrass at two sites in northern Puget Sound. U.S. Geological Survey Scientific Investigations Report 2008-5009, Washington URL. http://pubs.usgs.gov/sir/2008/5009/.

Stride, A.H., 1963. Current swept sea floors near the southern half of Great Britain. Q. J. Geol. Soc. Lond. 119, 175–199.

Stuiver, M., Reimer, P.J., 1993. Extended 14C database and revised CALIB radiocarbon calibration program. Radiocarbon 35, 215–230.

Syvitski, J.P.M., Vörösmarty, C.J., Kettner, A.J., Green, P., 2005. Impact of Humans on the Flux of Terrestrial Sediment to the Global Coastal Ocean. Science 308 (5720), 376–380.

Syvitski, J.P.M., Kettner, A.J., Overeem, I., Hutton, E.W.H., Hannon, M.T., Brakenridge, G.R., Day, J., Vorosmarty, C., Saito, Y., Giosan, L., Nicholls, R.J., 2009. Sinking deltas due to human activities. Nat. Geosci. 2 (10), 681–686. ISSN 1752-0894. https://doi.org/10.1038/ngeo629.

Toft, J.D., Munsch, S.H., Cordell, J.R., Siitari, K., Hare, V.C., Holycross, B., DeBruyckere, L.A., Greene, C.M., Hughes, B.B., 2018. Impact of multiple stressors on juvenile fish in estuaries of the Northeast Pacific. Glob. Chang. Biol. 24, 2008–2020.

Tucker, D.S., Scott, K.M., Grossman, E.E., Linneman, S., 2014. Mount Baker lahars and debris flows, ancient, modern, and future. In: Dashtgard, S., Ward, B. (Eds.), Trials and Tribulations of Life on an Active Subduction Zone: Field Trips in and around Vancouver. Canada, Geological Society of America Field Guide, pp. 33–52. https://doi.org/10.1130/2014.0038(03).

Tyler, D.J., Danielson, J.J., Grossman, E.E., Hockenberry, R.J., 2020. Topobathymetric Model of Puget Sound, Washington, 1887 to 2017. U.S. Geological Survey data releasehttps://doi.org/10.5066/P95N6CIT.

U.S. Coastal and Geodetic Survey, 1891. Hydrographic Survey 2050 of Skagit Bay and Vicinity Descriptive Report. https://www.ngdc.noaa.gov/nos/H02001-H04000/H02050.html.

Van Veen, J., 1935. Sandwaves in the North Sea. Int. Hydrogr. Rev. 12, 21–29.

Vörösmarty, C.J., Meybeck, M., Fekete, B., Sharma, K., Green, P., Syvitski, J.P.M., 2003. Anthropogenic sediment retention: major global impact from registered river impoundments, Global and Planetary Change. Vol. 39 (1–2), 169–190.

van der Wal, D., Lambert, G.I., Ysebaert, T., Plancke, Y.M.G., Herman, P.M.J., 2017. Hydrodynamic conditioning of diversity and functional traits in subtidal estuarine macrozoobenthic communities. Estuar. Coast. Shelf Sci. 197, 80–92.

Wang, H., Yang, Z., Saito, Y., Liu, J., Sun, X., Wang, Y., 2007. Stepwise decreases of the Huanghe (Yellow River) sediment load (1950–2005): Impacts of climate change and human activities. Glob. Planet. Chang. 57 (3-4), 331–354. https://doi.org/10.1016/j.gloplacha.2007.01.003.

Wang, H., Yang, Z., Wang, Y., Saito, Y., Liu, J., 2008. Reconstruction of sediment flux from the Changjiang (Yangtze River) to the sea since the 1860s. J. Hydrol. 349 (3-4), 318–332. https://doi.org/10.1016/j.jhydrol.2007.11.005.

Webster, K.L., Ogston, A.S., Nittrouer, C.A., 2013. Delivery, reworking and export of fine-grained sediment across the sandy Skagit River tidal flats. Cont. Shelf Res. 60S, S58–S70.

Weston, N.B., 2014. Declining sediments and rising seas: an unfortunate convergence for tidal wetlands. Estuar. Coasts 37, 1–23.

Wright, S.A., Schoellhamer, D.H., 2004. Trends in the sediment yield of the Sacramento River, California, 1957-2001. San Francisco Estuary Watershed Science 2 (2), 14.

WSU, 2014. http://extension.wsu.edu/skagit/wp-content/uploads/sites/29/2014/02/WSU-Skagit-County-Agricultural-Statistics-2014.pdf.

Wu, X., Wang, H., Bi, N., Saito, Y., Xu, J., Zhang, Y., Lu, T., Cong, S., Yang, Z., 2020. Climate and human battle for dominance over the Yellow River's sediment discharge: From the Mid-Holocene to the Anthropocene. Marine Geol. 425, 106188.

Ysebaert, T., Herman, P.M.J., 2002. Spatial and temporal variation in benthic macrofauna and relationships with environmental variables in an estuarine, intertidal soft-sediment environment. Mar. Ecol. Prog. Ser. 244, 105–124.

Ysebaert, T., Herman, P.M.J., Meire, P., Craeymeersch, J., Verbeek, H., Heip, C.H.R., 2003. Large-scale spatial patterns in estuaries: estuarine macrobenthic communities in the Schelde estuary, NW Europe. Estuar. Coast. Shelf Sci. 57, 335–355.

Zhao, Z., Sun, Z., Wang, Z., et al., 2013. The dynamic mechanism of post-rift accelerated subsidence in Qiongdongnan Basin, northern South China Sea. Mar. Geophys. Res. 34 (3–4), 295–308. https://doi.org/10.1007/s11001-013-9188-2.